THE USE OF A NEURAL NETWORK TO RECOGNIZE PLACENTAL INSUFFICIENY FROM BLOOD FLOW VELOCITY WAVEFORMS IN THE UMBILICAL CORD

by

Alkathafi Ali Alhamud

Submitted to the University of Cape Town
In partial fulfilment of the requirements for the degree of
Master of Science in Medicine
In the field of Biomedical Engineering

December 2004

Abstract

Present-day obstetric decision- making is based on measuring the umbilical arterial blood flow velocity waveforms from one site of the cord. There is an ongoing debate on the predictive value of Doppler measurements in the evaluation of the foetal condition.

The aim of this thesis is to investigate the use of a neural network to recognise blood flow waveform shape patterns associated with placental insufficiency. Eleven backpropagation neural networks have been developed and trained based on the waveforms that are generated from the foetal mathematical model (developed in previous research) at both ends of the cord. Only two networks trained successfully. These two networks are the Levenberg-Marquardt algorithm (Trainlm) and the resilient backpropagation algorithm (Trainrp). We observed that training the neural network from one site of the cord is impossible. It was therefore necessary to use other locations for the networks to be trained successfully. The trained neural network predicted the physiological patterns that are associated with each umbilical waveform. Then the need was to find a way to interpret these patterns for improved evaluation of the foetal condition. The centile graphs were therefore generated.

Thereafter, 29 unseen clinical waveforms were presented to the trained neural network in order to test it. We observed the following from the analysis of clinical data by neural networks: (1) Resistance index 'RI' would be high if the umbilical radius was high and the placental resistance was normal; (2) RI would be predominantly high if the placental resistance was high; and (3) Surprisingly, in some cases, RI would be normal if the placental resistance was high and the umbilical radius was small. We conclude that measurements of the umbilical blood flow velocity waveform at both ends of the cord together with umbilical radius represent a significant indicator in identifying the true foetal condition.

Declaration

I declare that *the use of a neural network to recognize placental insufficiency from blood flow velocity waveforms in the umbilical cord* is my work, and has not been submitted for any degree or examination in any other university. All sources I have used or quoted have been indicted and acknowledged by complete references,

Full name Alkathah Ali Alhamid Date 13-12-2004

Signed..... Signed by candidate

ACKNOWLEDGMENTS

I would like to express my profound appreciation to the following people, all of whom have been uniquely instrumental in the culmination of this project.

- Allah, the Most Gracious and the Most Merciful

- Dr Wayne Capper, who served as my supervisor, his commitment to this project was a constant source of inspiration from its initial stages to completion.

- Professor Kit Vaughan, for acting as co-supervisor to my work, whose meritorious dedication to this department served as a consistent impetus.

- Mr Andre Bester, whose suggestions relating to neural networks led the project to fruition.

- The Staff of the Department of Biomedical Engineering at The University of Cape Town, for their support offered to all students.

- The staff of the Department of Obstetrics and Gynaecology, Tygerberg Hospital, Cape Town.

- The staff of both the medical and main campus libraries of The University of Cape Town, which offered friendly and efficient assistance at all times.

- Mrs Anet Potgieter from The Faculty of Computer Science at The University of Cape Town who offered assistance pertaining to neural networks.

I dedicate this modest work to my country, The Great Socialist People's Libyan Arab Jamahiriya and the Libyan People Bureau in Pretoria, South Africa, in particular Dr Abdullah Abdu Salaam Zubaidi , who offers support and encouragement to all Libyan students in South Africa. To whom I am grateful for their significant financial contributions to my studies.

I dedicate this work to the following people:

My father , the late Mr Ali A. Alhamud, completed shortly after his passing.
My mother, her lifelong support and love serving to realise this work.
My brothers, sisters and friends.
Mrs Aishah Rogers, her son Jibreel and her father Mr Frederick Charles Rogers, who have been most helpful.

List of Contents **Page**

List of Figures **Page**

Figure **Page**

List of Tables **Page**

List of Equations **Page**

Equation **Page**

Chapter 1. Introduction

The foetus is dependent on blood flow through the placenta for nutrient and oxygen supply and for the elimination of all waste products. If the placental circulation is impaired (placental insufficiency), the foetus may suffer retarded growth, and, in extreme cases, it may suffer organ and brain damage. Small size for gestational age is a risk factor. It is, however, necessary to be able to distinguish between naturally small foetuses and those with placental insufficiency.

Placental insufficiency is thought to be associated with a decrease in the number of small muscular arteries in the placental tertiary stem villi (Giles et al. 1985a, Giles et al. 1985b). These morphological changes may adversely affect the oxygen supply and transport of nutrients.

It is common practice to use Doppler ultrasound to obtain umbilical cord flow waveforms. The umbilical cord, which contains the arteries that supply the placenta with blood is about 45cm long at 28 weeks and lengthens as gestation progresses. In cases of placental insufficiency, flow waveforms in the umbilical cord are known to have a different shape (compared to normal). Flow waveforms in the cord have thus been used clinically; both as an early warning system and to quantify placental insufficiency. There is nothing novel about this. Clinical decisions, nonetheless, are seldom performed on the basis of cord blood flow waveforms. One of the reasons for this is that factors other than placental insufficiency affect the shape of the cord flow waveforms, and this may result in false positives, or worse, false negatives.

It is important to establish which physiological changes alter the waveform shape if Doppler ultrasonography is to become a useful technique for assessing the foetal condition.

Since the effects of the various factors contributing to placental insufficiency are difficult to investigate clinically, previous work (Myers 2001; Capper and Myers 2003) focused

on developing a mathematical model of the foetal circulation, which could be used to theoretically investigate the important factors affecting cord flow waveform shape. From the thousands of possible factors, they were able to exclude most as having a negligible effect. However, they also identified those that are important, and it is these factors on which the present research will be concentrated. Furthermore, these authors noticed that the flow waveform-shapes at either end of the cord have a slight but consistent difference figure (1-1). This difference changes with modifications to the physical properties of the model, including placental insufficiency.

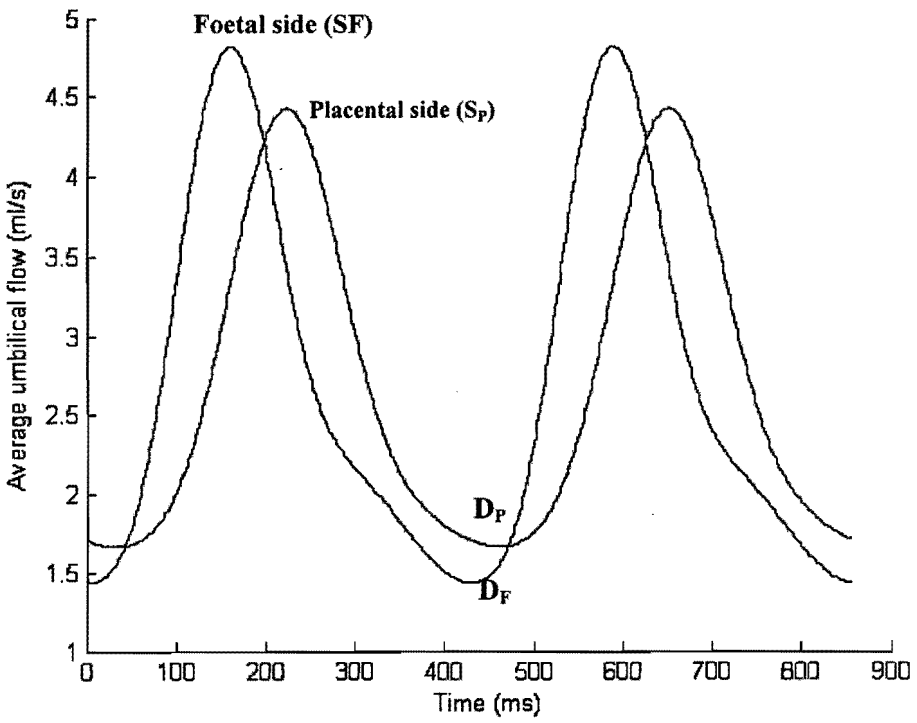

Figure (1-1): Umbilical arterial flow waveforms at both ends of the cord generated from the foetal model

S: maximum systolic velocity.

D: maximum diastolic velocity.

Even though they identified the most important factors affecting the shape of the umbilical blood velocity waveform, it is no straightforward matter applying this to clinical practice. What we need is a way in which we can measure the flow velocity waveforms and then extract from these the important factors affecting their shape. This is where neural networks could prove useful.

1-1 The Aims of this Thesis

1- To investigate the use of the neural network as an agent for recognizing patterns in blood flow velocity waveforms that are associated with both placental insufficiency and normal placental function.
2- To investigate the effect of the sampling site on blood flow velocity waveforms.
3- To study the effects of the physiological and anatomical factors, in particular the umbilical radius and placental resistance, on the umbilical blood flow velocity waveforms.

1-2 Clinical Investigation for Placental Insufficiency

1-2-1 Placental Insufficiency

The placenta (expelled post- natally and commonly referred to as afterbirth) is a thick, spongy, disc-like organ that develops in the uterus during pregnancy. At its full size it is approximately 20cm in width and 2.5 cm thick. The placenta is responsible for supplying the developing foetus with oxygen and nutrition. Until recently, doctors thought that it was the placenta that was to blame for foetal malnutrition resulting in intrauterine growth retardation. 'Placental Insufficiency' is therefore, the term used by doctors to describe the condition in which placental function falls short of meeting the foetus's nutritional requirements that are essential to growth.

Inadequate functioning of the placenta was furthermore thought to be the cause of conditions such as 'Foetal Distress' and 'Hypoxia'.

Intrauterine Growth Retardation and Foetal Distress are both grave conditions that could lead to the death of the foetus if left unchecked. Scientific research has been performed in an attempt to establish the causes of and preventative measures for Intrauterine Growth Retardation and Foetal Distress.

In an attempt to detect placental insufficiency, doctors have measured maternal blood levels for various substances produced by the foetus and placenta. Despite their usefulness, these tests are often unreliable and misleading in their results.

A special technique known as the Doppler Ultrasound Scan allows doctors to measure the flow of blood to the placenta and thereby establish the existence of anomalies at a very early stage.

1-2-2 Doppler in Foetal Medicine

Doppler ultrasonography is considered to be a major advance in obstetrics and perinatal medicine. It is a simple, non-invasive procedure that is applied to the study of foeto-placental blood flow in the human foetus. Prior to the advent of Doppler ultrasonography, invasive animal experiments were the prime source of knowledge about foeto-placental blood flow.

1-2-3 Waveform Analysis

One way in which Doppler waveforms can be analysed is to look at the relationship between the mean systolic and diastolic blood velocity waveform components. The most common indices are the pulsatility index (PI= (peak systolic velocity – end diastolic velocity) / (time-averaged velocity over the cardiac cycle)), the resistance index (RI = (peak systolic velocity – end diastolic velocity) / (peak systolic velocity)) and S/D (systolic / diastolic ratio) . These indices are called Doppler indices 'DI'.

1-2-4 The Dilemma of Doppler in Foetal Medicine

Perinatal surveillance is conducted, to a large extent, by monitoring the uterine artery, various foetal vessels and the umbilical artery blood flow velocity waveforms (Ruissen et al. 1990). The use of Doppler technology in Perinatal medicine has become routine, however, little progress has been made regarding interpretative methodologies surrounding its use. Clinically applied, a number of arteries and Doppler indices are used although their predictive values in foetal surveillance are not yet clear (Maulik et al. 1990). Physiological and pathological reasons for the altered Blood flow velocity waveforms, BFVW's both in normal and abnormal foetal growth are also still unclear (Beksac et al. 1995).

Although umbilical artery velocity indices are commonly abnormal in foetuses with growth retardation, Doppler ultrasound has proved disappointing as a screening test for this condition (Beattie et al. 1989).

A study of women with pre-eclampsia, also known as pregnancy-induced hypertension, showed that 70% had normal umbilical artery indices with no clear correlation between the Doppler indices and level of hypertension (Cameron et al. 1988).

Another issue, proving that the present way, in which Doppler ultrasound is used, is not a good screening tool in foetal medicine, is the location of the measurements. Waveforms that are generated along the umbilical artery are not uniform .A study of the variability of the umbilical artery S/D ratios along the umbilical cord (Helen et. al.1989) demonstrates a trend for S/D ratios to be lowest at the placental origin and highest at the foetal abdominal wall. The aetiology of this non-uniformity is unknown.

(Sonesson et al. 1993) concluded that routine recordings for Doppler indices should take into account the recording site on the umbilical cord in order to reduce methodological sources of variance, especially during mid-gestation.

These contradictions regarding the use of Doppler ultrasound as a screening tool in the evaluation of foetal conditions led many researchers to try to improve Doppler analysis either by using mathematical models, which simulate the foeto-placental circulation or by developing new indices instead of the conventional ones (RI, PI and S/D). More recent advances have seen a neural network method being used as a diagnostic system for the interpretation of blood flow velocity waveforms. These mathematical or animal models (sheep) are developed to allow us to understand the effect of various physiological patterns on the blood flow velocity waveforms in the umbilical artery.

The use of the neural network in the interpretation of the umbilical blood flow velocity waveform is not a new technique. The uniqueness of this project is the fact that two techniques will be employed. The first being the foetal mathematical model which has already been developed in a previous project (Myers 2001; Capper and Myers 2003) and the second is the use of the neural network to quantify the affect of the physiological factors on the shape of blood flow velocity waveforms.

This combination has enabled us to understand effects, which are usually quite difficult to comprehend or notice using normal programmatic computer logic or the human brain alone.

1-2-5 Why use the Neural Network in Particular?

It is quite difficult to obtain Doppler waveforms from the foetus with its changing physiological factors because there are thousands of different combinations of physiological factors, each having an associated BVW shape.

It therefore became necessary to create a mathematical model that would simulate the foetal circulation and accommodate changes in these factors as far as possible.
This model can be used to generate waveforms. Given the physiology of the foetal circulation, we can obtain large numbers of waveforms from the umbilical-placental circulation. Each waveform can then be associated with a set of physiological factors.

It might be that there is an algorithm, which correlates the Doppler indices with physiological factors. It is worth noting that there is some research, which showed linear regression correlation between the Doppler indices and the foetal heart rate (Mulders 1986; Mires et al. 1987; Yarlagadda et al. 1989). In reality this kind of correlation (linear regression) does not show the real relationship. So we cannot use or rely on the linear-correlation analysis in our study.

A more powerful system is needed that can be used to extract information or draw a map to describe the relationship between the Doppler indices' values and their corresponding physiological factors. This is where Neural Networks, could prove useful.
Because neural networks have a remarkable ability to derive meaning from complicated or imprecise data, they can be used to extract patterns that are too complex to be noted by either humans or other computer techniques. (Stergiou and Siganos, 1996).

This is especially helpful with sensory data, or with data from complex processes such as medical data. An algorithm may exist, but is unknown or has too many variables. It is easier to let the neural network learn from examples. A problem with neural networks is that they have to be trained using examples of waveforms from all possible clinical scenarios, and this is not practical. However, it may be possible to train a neural network using the foetal model, as this can be used to generate large numbers of different waveforms very quickly.

1-3 Methodology

The basic methods, which have been followed in this thesis, are summarised briefly in three steps:

1-3-1 The First Step: The Foetal Model (already developed in a previous project)

The umbilical arterial (UA) blood flow velocity waveform is characterised by various indices, such as the UA Resistance index (RI). The assumption is that RI is affected by

the placental impedance, and can thus be used clinically to predict placental insufficiency. However, factors other than placental impedance also affect the RI. A mathematical model based transfer function has been used to investigate other factors, which affect the shape of the UA flow waveform, and hence the RI. From thousands of physiological and anatomical factors the model allowed identification of the most important factors that have a predominant effect on the shape of waveforms (see appendix D).

1-3-2 The Second Step: The Neural Network Technique

The data, generated from the previous mathematical model, is divided into two classes. The first class is the input set. This set consists of Doppler indices at the placental and the foetal side of the umbilical artery as well as foetal heart rate and gestational age (GA in weeks). The second class is the output set. This set consists of the physiological factors, which were used to generate each waveform.

We need to choose a particular type of neural network to present the input and output classes to. If successful, the result will be that it can identify the main physiological factors that affect the shape of the waveform.

There are many types of neural networks. The main ones are, 'supervised learning' and 'unsupervised learning'. In supervised learning, there is a "teacher" who, in the learning phase, "tells" the network what the correct behaviour would have been ("supervised learning"). Unsupervised rules do not require teachers because they produce their own output, which is then further evaluated.

We will only consider supervised learning in this research, and in particular, only one kind of training algorithm will be considered, that being the 'Back-Propagation algorithm'. The reason for choosing this algorithm is that any network structure can be trained with back-propagation when the desired output patterns exist (Supervised

learning) and each function that has been used to calculate the actual output patterns is differentiable.

The following lines summarise the steps, which have been taken in training the neural network see also figure (1-2).

1. By changing various physiological patterns, the foetal model is run repetitively to generate corresponding waveforms at either end of the cord.
2. Extract unique information from the waveforms (i.e. Doppler indices: RI and PI).
3. Choose the type of neural network that is most applicable to the foetal model.
4. Train the neural networks based on the foetal model data.

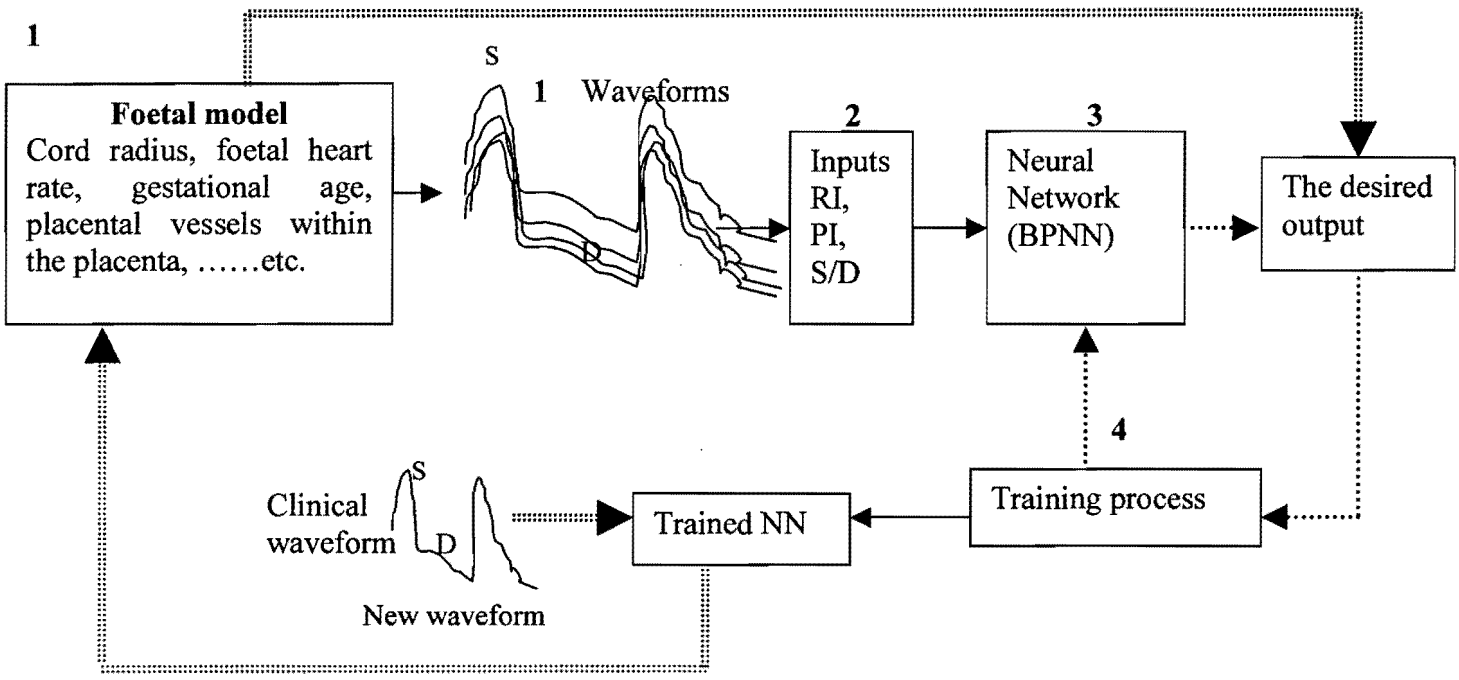

Figure (1-2) : Summary of the main steps taken with the neural network

1-3-3 The Third Step: Clinical Data

New clinical waveforms are presented to the trained neural network figure (1-2). This will allow us to assess whether the neural network is able to distinguish between various clinical scenarios. For this step we need to obtain umbilical flow velocity waveforms from the extremities of the cord, in a few selected patients. The foetal heart rate, gestational age and cord radius will also be recorded from the clinical data.

Chapter 2. Literature Review: Methodology of Doppler Assessment of the Foetal Circulation

This literature review covers a number of areas of interest:

1- We will firstly consider a serious problem concomitant with pregnancy: Placental Insufficiency with its causes and consequences.
2- We will consider the development of foeto-placental and utero-placental circulation during pregnancy.
3- We will consider a non-invasive technique using Doppler ultrasound to measure Placental Insufficiency.
4- We will consider Doppler ultrasound analysis of umbilical blood flow velocity waveforms (BFVWs).
5- We will consider some mathematical models, which have been introduced in order to achieve an understanding of the relationship between Doppler indices and flow impedance.

2-1 Placental Insufficiency

2-1-1 Definition of Placental Insufficiency

Progressive deterioration in placental functioning and a decrease in trans-placental oxygen and nutrient supply to the foetus is known as Placental Insufficiency .The major result of this condition is foetal hypoxemia (Lackman et al. 2001; Gagnon 2003). This happens due to the metabolic demands of the growing foetus. While premature birth is the primary cause of perinatal death, placental insufficiency, leading to Foetal Growth Retardation (FGR) is the second. It can complicate as many as 4-6% of all pregnancies. The perinatal mortality rate of FGR foetuses is 5 times higher than that of 'normal' foetuses. There is also a threefold greater risk of spontaneous pre-term delivery for FGR foetuses. At present, no treatment for FGR exists (caesarean section can reduce the risk) and 50% of incidences constitute cases where foetuses either die in utero, or are diagnosed post-natally. Infants who survive the perinatal period are nevertheless

predisposed to suffering cognitive deficiency. Evidence of this deficiency becomes apparent at school-going age. It is, furthermore, highly probable that certain health problems during both childhood and adulthood are caused by poor function of the placenta (Gagnon R. 2003).

We can therefore conclude that Placental Insufficiency is brought about by the failure of the placenta to develop and to act as it should. In consequence, the foetus does not grow and develop normally .The earlier in pregnancy that it occurs, the worse the consequences will be. Furthermore, FGR will occur if placental insufficiency extends over a long period in pregnancy.

2-1-2 The Causes of Placental Insufficiency

Let us now review the causes and related consequences of Intrauterine Growth Retardation, as summarised by Evan and Eileen, (2001):

- Defects of the placental membranes
- Defects of the umbilical cord
- Abnormal implantation of the placenta in the uterus
- A break in the placental membrane that causes foetal blood to mix with maternal blood
- Rh incompatibility, a condition in which the maternal blood group is not compatible with the blood group of the foetus.
- Multiple births (twins, triplets et al)
- Previous low-birth-weight infant
- Chronic Hypertension
- Diabetes
- Severe Renal disease
- Heavy smoking
- Insufficient weight gain by the mother during pregnancy, defined as less than 4.5 KG

- Pre-eclampsia or Eclampsia. Conditions resulting in maternal hypertension
- High altitude
- Drug addiction, such as addiction to cocaine
- Anticoagulants such as Warfarin
- Immunosuppressive medications
- Positive HIV status of the mother (Human Immune Virus)
- Alcohol abuse
- Infection caused by Cytomegalovirus, Toxoplasmosis, Rubella, or Syphilis, known collectively as TORCH infections
- Poor nutrition of the mother
- Infant with known birth defects or chromosomal abnormalities
- Frequent vaginal bleeding due to Placenta Praevia, a condition in which the placenta is attached to the uterus over or near the cervix
- Certain blood disorders in the mother, such as Sickle Cell Anaemia or Thalassaemia
- Premature placental separation, known as 'placental abruption'

2-1-3 The Consequences of Placental Insufficiency

Placental Insufficiency poses a host of risks to the foetus, at parturition and post-natally. These risks include the following:

- An 8-fold higher risk of death during delivery
- A 5-fold higher risk of poor oxygenation at birth that may lead to Cerebral Palsy and other complications
- Hypothermia, or low body temperature
- Hypoglycaemia, or low blood sugar
- 30% to 40% chance of learning disabilities
- Premature delivery
- Poor tolerance of labour
- Increased chance of Caesarean delivery
- Increased chance of birth defects

- Increased chance of Meconium aspiration during labour, in which the baby inhales some of the brown semi-fluid material that collects in its bowels pre-natally.
- Hypocalcemia, too little calcium in the blood

Placental Insufficiency carries with it serious, long- term effects for the neonate.

- The infant will tend to remain physically small post –natally
- There is a higher risk of neurological and intellectual impairment.
- Major disabilities include severe mental retardation, Cerebral Palsy and seizures

In an attempt to detect Placental Insufficiency, doctors have measured maternal blood levels for various substances produced by the foetus and placenta. Despite their usefulness, these tests are often unreliable and misleading.

A special technique known as the Doppler Ultrasound Scan allows doctors to measure the flow of blood to the placenta and thereby establish the existence of anomalies at a very early phase of pregnancy.

Before considering the use of Doppler ultrasound to measure Placental Insufficiency, we need to take into account the importance of describing how normal placental circulation develops during pregnancy, in other words, how blood flow changes within the placenta during normal pregnancy.

2-2 The Development of the Utero-Placental and the Foeto-Placental Circulation

The maternal cardiovascular system undergoes enormous change in pregnancy. To be specific, a low-resistance, high flow placental vascular bed develops. This vascular bed is unique in that it is composed of a maternal and a foetal component. Several cell layers that differ, depending on the species under consideration, separate its components. Evidence suggests that these two components function and respond independently of

each other, even though they are closely related in all species (Ehrenkranz 1976; Rosenfeld 1992).

It is vital to understand the controlling mechanisms of vascular tone because the placental blood volume flow rate relates to the delivery of oxygen and /or nutrients to the foetus as well as removal of carbon dioxide and other wastes. Any change in maternal or foeto-placental blood supply could modify the aforementioned transportation of nutrients and waste removal.

Accordingly, the reliability of the Utero-placental and Foeto-placental vascular bed is vital to the overall growth and development of the foetus.

2-2-1 The Development of the Utero-Placental Circulation

The uterine arteries constitute the principal supply of blood to the uterus, with the ovarian arteries serving as a secondary source to a much lesser degree. These vessels anatomise at the cornu of the uterus and give rise to arcuate arteries that run circumferentially round the uterus. The radial arteries arise from the arcuate vessels and penetrate at right angles into the outer third of the myometrium. These vessels then give rise to the basal and spiral arteries, which offer nourishment to the myometrium, decidua and the intervillous space of the placenta during pregnancy, respectively (Ramsey et al. 1963; Body et al. 1970) figure (2-1).

The respiratory and nutritional needs of the foetus and placenta demand that blood flow to the uterus increase by 10 times. In order for this to occur, spiral arteries have to undergo certain physiological changes. One of these physiological changes is an increase in the diameter of the spiral arteries, from 15–20 to 300–500 μm (Pijneborg et al. 1983). Therefore, impedance to flow is reduced and foeto-maternal exchange in the intervillous space is optimised.

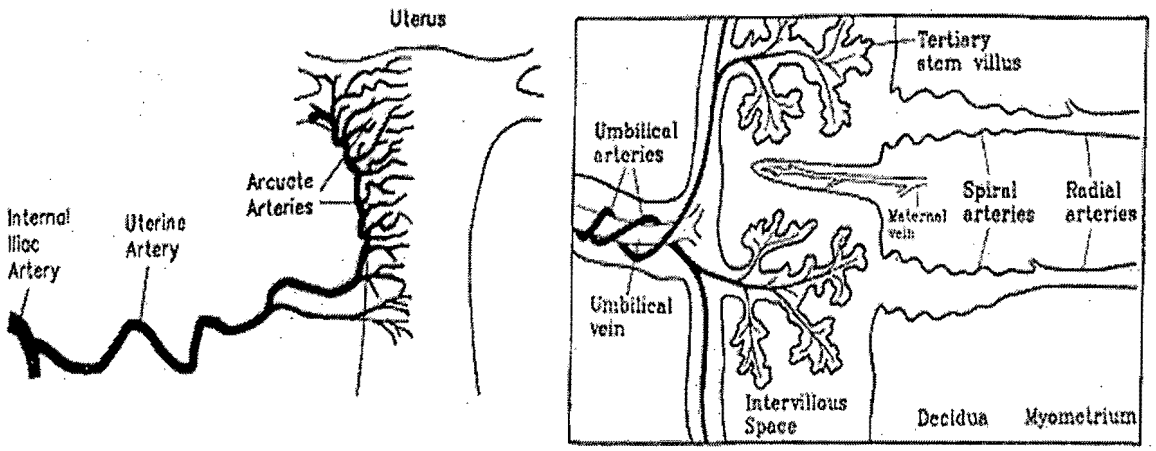

a b

Figure (2-1): Anatomical drawing of utero-placental vasculature (Larry et al. 1988): (a) the overall uterine arterial network, and (b) the details of the maternal-foetal interface system

2-2-2 The Development of the Foeto-Placental Circulation

Maternal utero-placental circulation has been widely studied and we now understand its functioning and anatomy (Rosenfeld 1992) Nevertheless, the patterns of change that occur in foeto-placental blood flow over the entire period of gestation, is something that few researchers have touched on.

It is clearly difficult to execute foeto-placental studies, even in an animal model. In humans, stem villi originate from the foetal side of the placenta. These stem villi branch from the umbilical artery and vein figure (2-2). As pregnancy progress, a villous tree and vascular bed develop from each stem villous, which subdivides, branches, and grows throughout pregnancy. In this manner, an ever-increasing foeto-placental vascular bed is provided as pregnancy nears term.

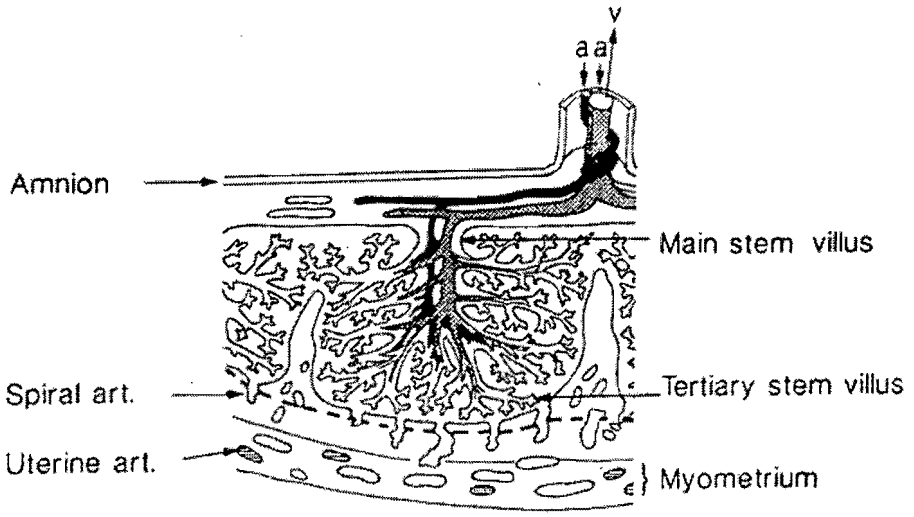

Figure (2-2): Section of the placenta showing the two umbilical arteries, first radial branches, and the branching villous tree (Rosemary et al. 1989).

Furthermore, Vascular impedance in the growing placenta decreases as the number of functioning vascular villi increases. This occurs from 20 weeks of gestation (Trudinger et al. 1985a).

Giles et al. (1985a, 1985b) reported that in foetal growth retardation due to placental insufficiency, there is obliteration of tertiary stem arterioles within the placenta that causes low diastolic flow relative to peak systolic flow.

2-3 Placental Insufficiency, Doppler Ultrasound and the Umbilical Artery

It is not yet known which mechanism is responsible for the decline in placental functioning which accounts for Placental Insufficiency. What is known is that certain risk factors on the part of the mother contribute to an increased risk of FGR. Umbilical arterial blood flow velocity can be measured to indirectly detect Placental Insufficiency by using Doppler Ultrasound (Trudinger et al. 1985b).

By measuring waveforms and finding abnormalities, foetuses that fall into the high risk category for perinatal death and long-term neurological complications can be identified. This reflects an increase in the umbilical-placental vascular resistance, which leads to a reduced umbilical blood flow (Trudinger et al. 1996; Gagnon et al. 1996).

A reduction in umbilical blood flow can be due to a decrease in utero-placental blood flow, abnormal villous structure at the interface between the maternal and foetal circulation, or a primary abnormality in the umbilical-placental perfusion (Salafia CM. 1997; Salafia et al. 1997).

2-3-1 Characteristics of the Umbilical Artery Flow Velocity Waveform

The umbilical artery was the first foetal vessel to be evaluated by Doppler velocimetry. Flow velocity waveforms of the umbilical artery are saw-tooth in appearance. The continuous wave Doppler examination of the umbilical artery is not a complex process. Peripheral arterial waveforms typically have a triphasic shape, but this is not evident in waveforms from the umbilical arteries. Which are more simplistic than seen in the foetal aorta. (Marsal et al. 1984; Griffin et al. 1984).

Characteristic waveforms from the umbilical artery are obtained by placing a transducer, which is usually pencil-shaped, on the abdomen of the mother, overlying the foetus. The transducer is then systematically manipulated to obtain the waveforms.

Furthermore, a Doppler scan, using a pulsed wave system, is conducted where the investigation of a free-floating section of cord is undertaken. Then the Doppler sample volume is placed over the umbilical artery, as shown in figure (2-3).

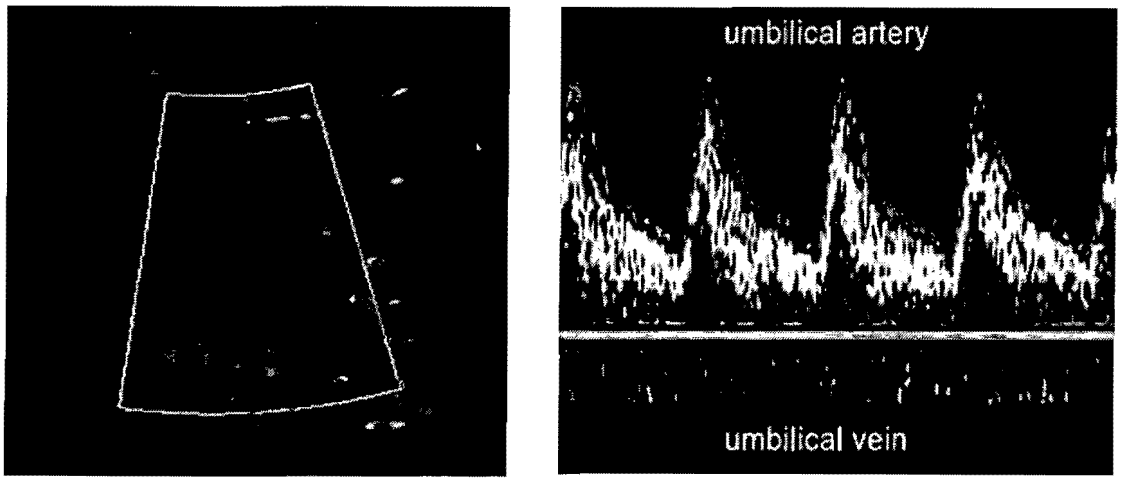

a b

Figure (2-3): (a) Ultrasound image with Doppler in colour showing the umbilical cord, red umbilical artery and blue umbilical vein. (b) Normal flow velocity waveforms can be seen from the umbilical vein (bottom) and artery (top) at 32 weeks of gestation (Kypros et al. 2001).

2-3-2 Doppler Analysis of Umbilical Artery Blood Flow Velocity Waveform

Calculating absolute blood flow in a vessel is challenging. It not only requires knowledge of the cross sectional area of the vessel (which changes with the cardiac cycle) but also necessitates that the ultrasound signal's angle of insonation with the vessel be known.

The blood flow velocity profiles across the cross-sectional area of the vessel, as well as the tissue density, that the ultrasound has to pass through to reach the vessel, have to be assumed.

Notwithstanding the requisite use of Duplex-pulsed Doppler equipment, significant errors in calculation of blood flow might occur (Stuart, 1992).

The fact that the maximum frequency outline of the flow velocity waveform provides a reproducible qualitative analysis of blood flow within the vessel is favourable.

2-3-3 Flow Waveform Shape: Indices of Measurement

Flow waveform shapes have been described using many different indices. A host of techniques is available; from simple indices of systolic to diastolic flow, to feature extraction methods such as principal component analysis. These techniques are designed to describe the waveform in a quantitative way, usually as a guide to some kind of classification. A compromise usually exists between simplicity and the amount of information obtained.

Most commercial scanners are equipped with the following commonly used flow indices:

(1) Resistance index (RI) also called Pourcelot's index.
(2) Systolic/diastolic (S/D) ratio, sometimes called the A/B ratio
(3) Pulsatility index (PI).

A description of how these indices are calculated is described in figure (2-4). The indices are independent of the intensity of the Doppler signal and the angle between the ultrasound wave and the vessel. In this way, it is possible to compare indices measured at different times and in different individuals.

When measuring the PI, one also has to measure the mean velocity of the waveform over a cardiac cycle. This means that it takes slightly longer to calculate than the RI or S/D ratio, although this is not really a factor, given the powerful computers of today. It also gives a wider range of values when, as an example, a range of waveform shapes are described where there is no end-diastolic flow.

For the most part, end-diastolic velocity influences quantitative Doppler flow indices such as the S/D ratio, resistance index (RI) or pulsatility index (PI). Very low end-diastolic velocities characterise abnormal foetal blood velocity waveforms. Noticeable changes in these quantitative indices take place due to miniscule modifications in velocity of the end-diastole velocity (Arduini et al.990).

The process of obtaining quantitative Doppler values, for example the maximum systolic, mean and the maximum end-diastolic velocity, is more complicated. This complexity arises because the examiner has to accurately position the angle between the Doppler beam and the blood vessel (Gill. 1985; Maulik et al 1989a) .

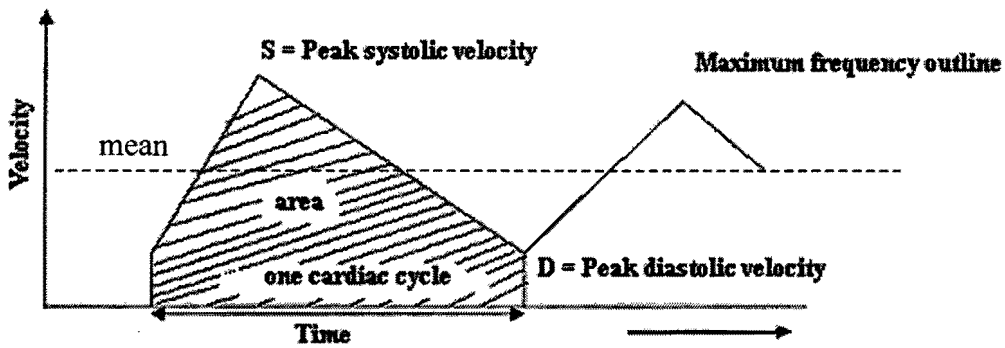

D: End diastolic velocity

mean = area / time.

- Pulsatility index (PI= (S-D)/mean).
- Resistance index (RI = (S-D)/S).
- and (peak systolic / peak diastolic) ratio = S/D.

Figure (2-4): Calculating typical Doppler indices

Hence, the volume of accessible information is reduced when using Flow indices to interpret Doppler results. However, there may be a discrepancy between Flow Indices and the actual clinical outcome.

When predicting complications such as IUGR or Foetal Distress, it is rare for quantitative Doppler indices to exceed 60% sensitivity and 90% specificity (Devoe et al. 1990).

There are no agreements as to the selection and calculation of the indices. Classical indices such as S/D ratio and RI have similarities in their parametric representation (Beksac et al. 1995). For these reasons, other indices have been introduced in an attempt to improve the usefulness of Doppler ultrasound as a diagnostic tool in obstetric management.

(Hendrik et al. 1996) proposed to create quantiles for utero-placental and foeta-placental blood flow velocity describing the development of peripheral vascular resistance during the third trimester. The aim of these new quantiles was to interpret the Doppler results in an improved manner by using both qualitative and quantitative indices. But in this study it was difficult to compare the quantiles' Doppler indices with other normal values obtained by other investigators.

Beksac et al. (1995), introduced new indices. These indices are entitled, the area ratio of wave (ARW) and angle between coincident slopes (ACS), as shown in figure (2-5). By also making use of an artificial neural network, they found that the predictive value of the system was satisfactory.

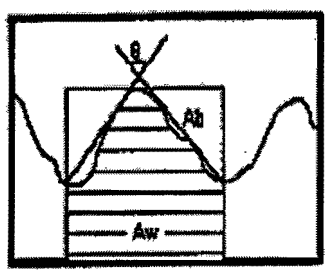

$$ARW = \frac{AW}{Ab}$$

$$ACS = \theta$$

Figure (2-5). Graphical representation of the new indices ARW and ACS (Beksac et al. 1995).

2-3-4 The Effect of the Sampling Site on the Umbilical Flow Velocity Waveform

The location of the Doppler sampling site in the umbilical cord influences the Doppler waveform. Measurements of placental indices, taken at the foetal end of the cord are significantly higher than those taken at the placental end. The reason for this might be that the foeto- placental vascular bed is a low impedance system that is associated with minimal wave reflection. This would explain the presence of a continuing forward flow in the umbilical artery during diastole (Maulik et al. 1990b).

In previous work (Jacques et al 1989), umbilical artery blood flow velocity waveforms at both ends of the cord were measured (i.e. placental insertion and foetal abdominal insertion). There was a significant statistical difference between the two sites. It was furthermore reported that normal values were obtained at the placental insertion, while the foetal abdominal insertion simultaneously generated highly abnormal values. It was concluded that abnormal values originating from foetal insertion should be treated with caution. They explained that, prior to entering the low-resistance network of the placenta, flow down the long tortuous umbilical vessels ranging between 30cm and 120cm in length, possibly influences Doppler indices at the foetal side.

Most of the debate in the literature has been concerned with the choice of a suitable site on the cord for measurement and clinical decision-making. There have not been any previous attempts to use the information from both ends of the cord in the decision making process. In subsequent chapters, this thesis will show that the difference in the flow indices at the ends of the cord contains information that's used to estimate the placental impedance.

2-4 Doppler Ultrasound in Normal and Abnormal Pregnancy

2-4-1 Doppler Ultrasound Of The Umbilical Arteries In A Normal Pregnancy

A high end-diastolic velocity characterises the umbilical arterial flow velocity waveform in normal pregnancy (figure 2-6). According to reports, this is more than half the systolic value (Surat and Adamson 1996) near full term . Many groups have published reference ranges for normal pregnancy. In normal pregnancy, flow indices decrease as gestation advances.

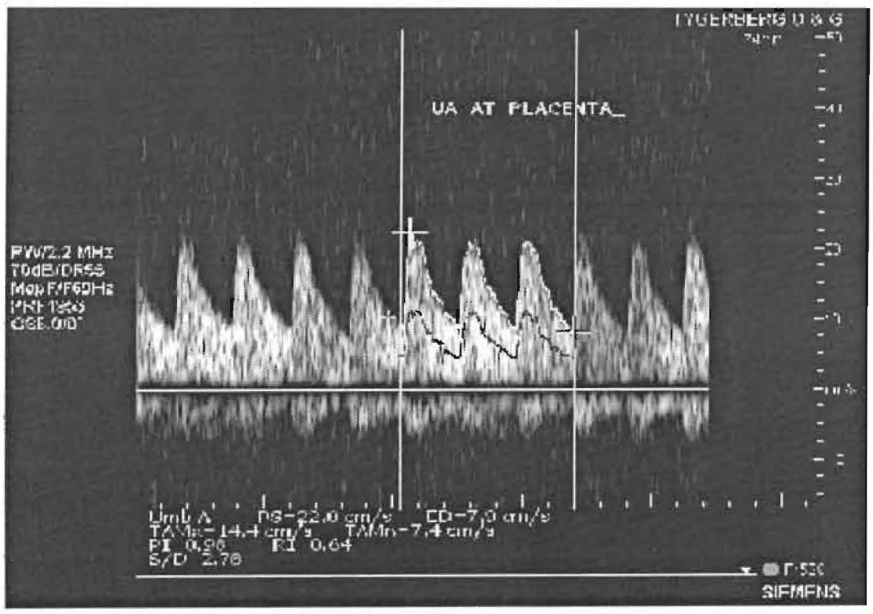

Figure (2-6): shows a normal pregnancy at gestation 36 weeks with normal diastolic velocity at the placental side. (Image recorded at Tygerberg Hospital, Cape Town).

2-4-2 Doppler Ultrasound of the Umbilical Arteries in an Abnormal Pregnancy

Where pregnancy becomes complicated by foetal compromise, the umbilical artery flow velocity waveform commonly has low or absent end-diastolic velocity (figure 2-7). This loss of end-diastolic velocity is thought to represent increased placental resistance (Erskine and Ritchie 1985a).

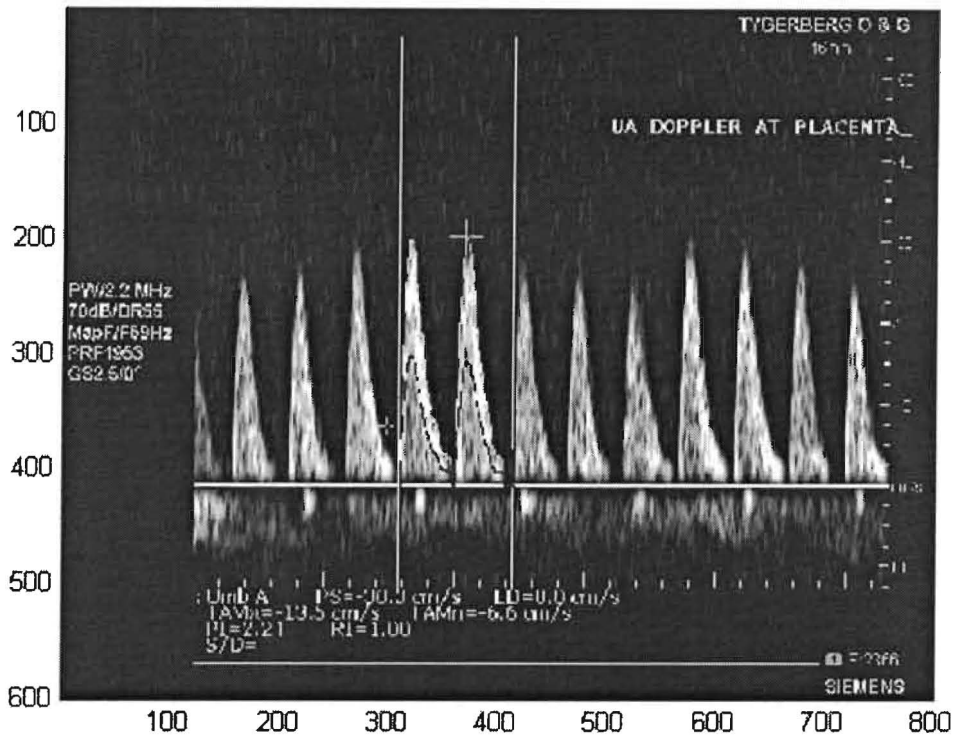

Figure (2-7): Abnormal umbilical Doppler waveform (28 wks) in a case of maternal Pre-eclampsia. Diastolic velocity at the placental side of the cord is absent. (image recorded at Tygerberg Hospital, Cape Town).

2-4-3 Doppler Ultrasound of the Umbilical Arteries and Intrauterine Growth Retardation (IUGR)

Reports of the association between IUGR and reduced or absent end-diastole in the umbilical arteries have been presented (Fleischer et al. 1985; Stuart 1992; Erskine and Ritchie 1985b). IUGR foetuses commonly present with abnormal umbilical artery velocimetry indices.

However, Doppler ultrasound screening has not proved useful as and indicator for foetal growth retardation. (Beattie et al. 1989).

2-4-4 Doppler Ultrasound of the Umbilical Arteries and Hypertensive Pregnancy

Women suffering from hypertension are inclined to display an increased incidence of reduced, absent, or even reversed end diastolic flow (Ducey et al 1987) (figure 2-8).

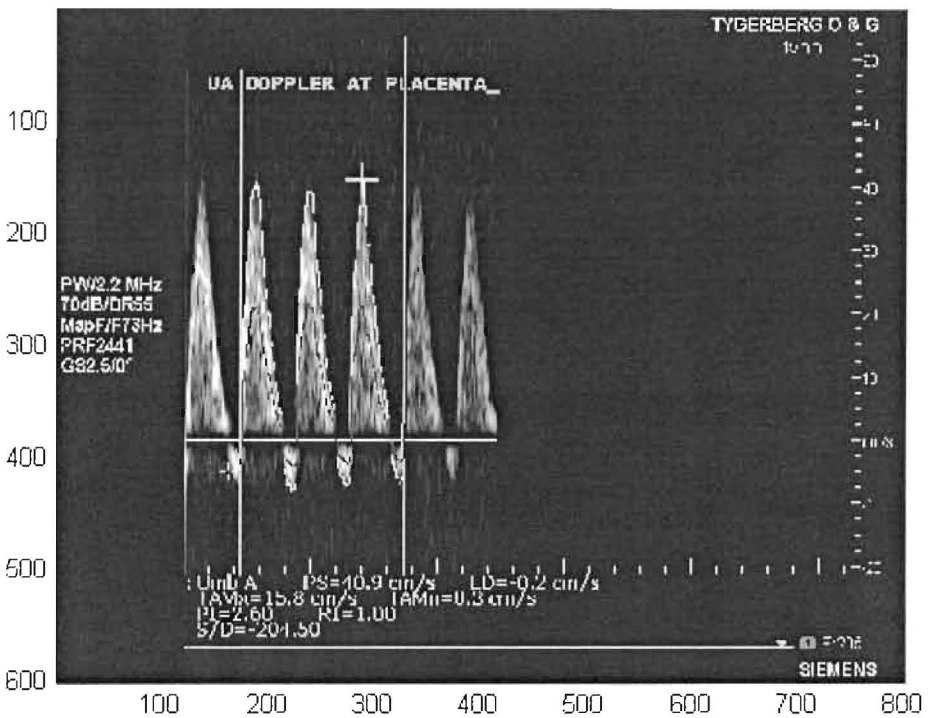

Figure (2-8): A 29 week old foetus presenting with abnormalities linked to Pre-eclampsia, and a resulting reverse diastolic velocity at the placental side . (image recorded at Tygerberg Hospital, Cape Town).

It was also demonstrated that abnormal Doppler indices are more common in women with gestational protein-uric hypertension than in woman with either gestational or chronic hypertension (Davey et al 1987). The typical placental vascular lesions of Pre-eclampsia, which are a common cause of gestational protein-uric hypertension, may be reflected in this. Retention of small high resistance maternal arterioles will be prevalent

too (Dixon et al 1958). This leads to ischaemia of the intervillous space and possibly spasm or occlusion of the foetal tertiary stem villi.

In a study of Pre-eclamplsia (Cameron et al. 1988) it was found that 70% of cases had normal umbilical artery indices with no clear correlation between Doppler indices and levels of hypertension.

2-5 Doppler Indices, Blood Flow and Impedance to Flow (Mathematical models)

Impedance is the ratio of the pressure to the flow, and is dependant on both the resistance and the reactance of the vessel wall. A lot has been learnt about the relationship of Doppler indices to flow and impedance from physical and animal models.

A model created by Erskine and Ritchie (1985b), was based on a phantom immersed in a bath of water. Citrated blood was then pumped through the system in a pulsatile manner. It was found that a linear relationship exists between true mean blood velocity and the average maximum Doppler shifted frequency.

A few years later, Thompson and Stevens (1989) devised an electrical circuit model of the branching patterns prevalent in the umbilical-placental circulation, in which each vessel was allocated resistance and capacitance values. The model indicated that the pulsatility index (PI) of the Doppler waveform depends both on the pulsatility of the input pressure waveform and on the ratio of the resistance of the placental vascular bed to the resistance of the umbilical artery.

An electrical analogue model of the umbilico-placental circulation was devised by Surat and Adamson (1996). This model was based on haemodynamic measurements in sheep foetuses. It was used to predict the mean blood velocity waveform in the umbilical artery.

Conclusions drawn by the group were that high placental resistance, low umbilical arterial resistance or a combination of these parameters, are the primary downstream determinants of elevated pulsatility in the umbilical arterial blood velocity.

Yet another mathematical model was introduced in by Ayala et al. (1999). This model was based on a haemodynamic model for pulsatile fluid flow. The volumetric blood flow and velocity profiles were computed for a pressurized thin walled elastic tube at any selected location. The simulated FVW allowed analysis of the sensitivity of DI to the site of Doppler measurements. The results revealed that DI are insensitive to the radial adjustment of the ultrasound beam as long as it is far away from the walls. However, the axial location affects the computed values of the DI, which supports the recommendations to measure DI at defined points (e.g. placental insertion). They furthermore demonstrated other results pertaining to blood and wall properties and the effects these had on the velocity profile.

2-6 Summary

The umbilical arterial blood velocity waveform is the product of complex physiological processes for which there is no complete mathematical model. Quantitative indices are used to infer information about physiological effects, but these are based on observation rather than theory and lack definitive physical interpretation. The exact relationship between different indices is usually not known and in some cases different applications have been suggested for the same index (Thompson et al. 1986).

Numerous researchers have made proposals on how to improve Doppler measurements, either by introducing new indices or by using mathematical models to analyse the commonly used indices. Although these models allow us to further understand the umbilical artery blood flow velocity waveform, the discrepancies between the umbilical waveform results and the clinical outcomes persist.

In the following chapters we will see how the combination of arterial blood flow velocity waveform indices, with their physiological and anatomical patterns, as well as a neural network, will allow us to understand things which had previously been difficult to understand or distinguish, either by the mathematical model itself or by the human brain.

Chapter 3. Literature Review: Neural Networks

This chapter is intended to review and aid the understanding of Artificial Neural Networks, how they work, and what the main considerations are for this project.

3-1 Introduction

Researchers have endeavoured to simulate biological neural networks by way of artificial neural networks (ANN). Artificial neural networks are, therefore, information processing systems. The field of ANN's developed out of the need to expand the abilities of the computer, which were limited, to execute certain functions. Tasks as straightforward to humans as reading handwritten documents or recognizing faces, pose a challenge to even the most sophisticated computer. As a result, programmers began entertaining the possibility of developing technology that would imitate the operations of the human brain, with its neurons and synaptic connections. (Hertz et al. 1991; Fausett 1994; Demuth et al. 1998; Samem et al. 2002).

3-1-1 What are Artificial Neural Networks?

The domain of Artificial Neural Networks is known by many names, such as connectionism, parallel distributed processing, neuro-computing, natural intelligent systems, machine-learning algorithms, and artificial neural networks (Klerfors 1998).

It is a system loosely modelled on the human brain, which attempts to simulate the multiple layers of simple processing elements called neurons by means of specialised hardware or sophisticated software. Each neuron is linked to a number of its neighbours with varying coefficients of connectivity representing the strengths of these connections. Learning occurs when these strengths are adjusted causing the overall network to output appropriate results.

3-1-2 Analogy to the Brain

In spite of being the focus of in-depth research, the brain and its performance largely remain enigmatic. Studies have nevertheless, been able to yield a certain understanding of the arrangement and processes within this phenomenal organ, in particular, the most basic element of the human brain, the neuron. The neuron is a specific type of cell, which appears to be different to cells in the rest of the body, in that it does not regenerate. It is therefore assumed that these cells provide us with the ability to remember, think, and apply previous experiences to everything we do. There are approximately 100 billion neurons in the human brain (Mcneill and Anderson 1992). Each neuron can connect with up to 200,000 other neurons, although the typical number is between 1,000 and 10,000. The titanic brainpower, peculiar to the human being, lies in the brain's immense number of basic components (neurons) and the multiple connections between them. Furthermore, genetic programming and learning contribute to man's mental prowess.

Individual neurons are complex in nature. They consist of an uncountable number of parts, sub-systems, and control mechanisms which all assist in conveying information via a host of electrochemical pathways. There are over one hundred different classes of neurons, depending on the classification method used. Together these neurons and their connections form a process that is neither binary, stable or synchronous. To be precise, the currently available electronic computers, or even artificial neural networks are nothing like it. These artificial neural networks primitively try to replicate only the most basic elements of this complicated, versatile, and supreme organ. However, for the software engineer trying to solve problems, neural computing has never been about replicating human brains but rather about machines and a new way of solving problems.

3-1-3 The Artificial Neuron

The fundamental unit of an organic neural network is the neuron. The neuron is the basic element of human consciousness and includes a few general capabilities. In essence, a biological neuron receives inputs from other sources, combines them in some way,

performs a generally non-linear operation and then outputs the final result (Klerfors 1998; Mcneill and Anderson 1992). Figure (3-1) illustrates the relationship between these four parts.

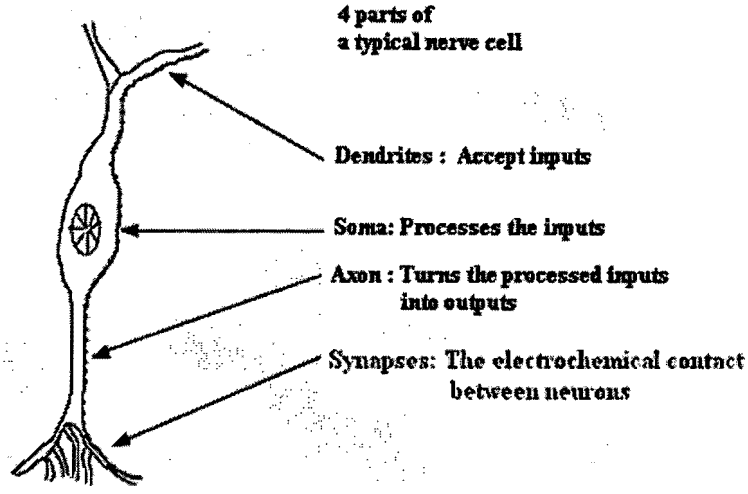

Figure (3-1): A biological neuron

Given the astounding intricacy of the human brain, it is not surprising that the complexity surrounding physiological neurons becomes highly abstract when modeling artificial neurons. However, it is worth noting that the neural network does not have, as its aim, the grandiose recreation of the brain. On the contrary, neural network researchers seek to understand the innate capacities that enable people to engineer solutions to problems that have not been solved by traditional computing. To do this, the basic unit of neural networks, the artificial neuron, simulates the four fundamental functions of biological neurons as shown in figure (3-1). Figure (3-2) illustrates a basic representation of an artificial neuron.

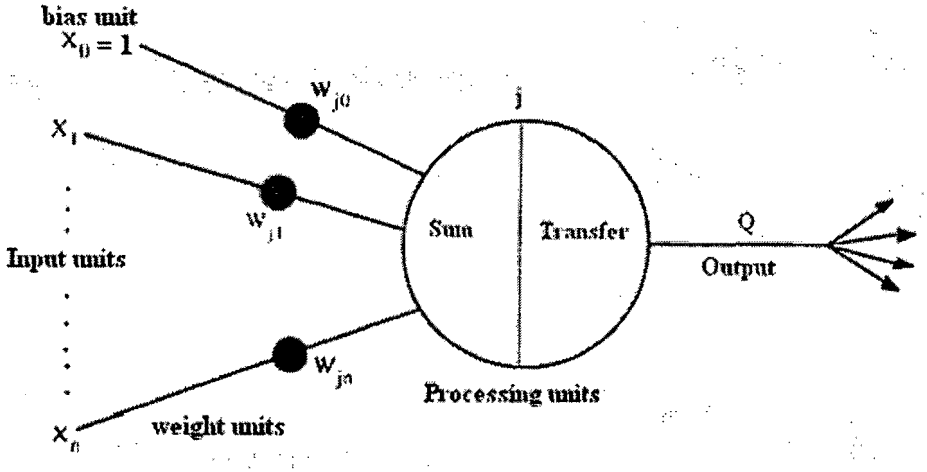

Figure (3-2) : An artificial neuron

In general terms the relationship between the inputs $x_0 \ldots x_n$, of neuron j and its output is given by equations (1) and (2). The output function is typically a non-linear function.

(Summation function) $A_j = \sum_{i=0}^{n} w_{ji} x_i$ 3-1

(Transfer function) $Q_j = f(A_j)$ 3-2

Each neuron is allowed one output signal, which may output to hundreds of other neurons figure (3-2). This just likes the biological neurons, where there are many inputs and only one output action. Normally, for the output function, the output is directly equivalent to the transfer function's result.

3-1-4 The Summation or Combination Function

As the inputs are presented to the neural network, the first step in a processing element's operation is to compute the weighted sum of all of the inputs. The summation function is found by multiplying each value of the input vector by the corresponding component of the weight 'w' (i.e. the strength of connection of the input to neuron j), and then adding up all the products as shown in equation (3-1).

3-1-5 Transfer Function

An algorithmic process called the transfer function transforms the result of the summation function to a working output, which is almost always the weighted sum. The activation level associated with each neuron is also the output value of each neuron. In the transfer function the summation total can be compared with some threshold to determine the neural output. If the sum is greater than the threshold value, the processing element generates a signal. If the sum of the input and weight products is less than the threshold, no signal, or some inhibitory signal, is generated.

The threshold, or transfer function, is generally non-linear. Linear or 'straight-line' functions are limited because the output is simply proportional to the input. Linear functions are not very useful.

The transfer function could be something as simple as depending upon whether the result of the summation function is positive or negative. The network could output zero and one, one and minus one, or other numeric combinations. The transfer function would then be a "hard limiter".

Another option would be a sigmoid or S-shaped curve. The curve approaches a minimum and maximum value at the asymptotes. It is common for this curve to be called a sigmoid when it ranges between 0 and 1, and a hyperbolic tangent when it ranges between -1 and 1. Mathematically, the exciting feature of these curves, as opposed to the hardlimiter, is that both the function and its derivatives are continuous. (Dayhoff 1990; Mcneill and Anderson 1992) This option works fairly well and is often the transfer function of choice see Figure (3-3) for sample transfer functions.

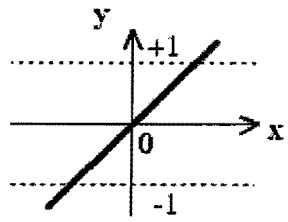

Linear transfer function

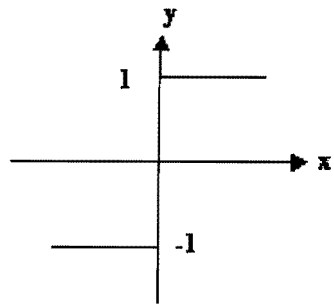

Hard Limiter transfer function

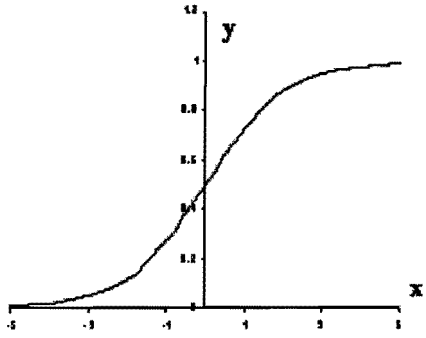

Log-Sigmoid transfer function

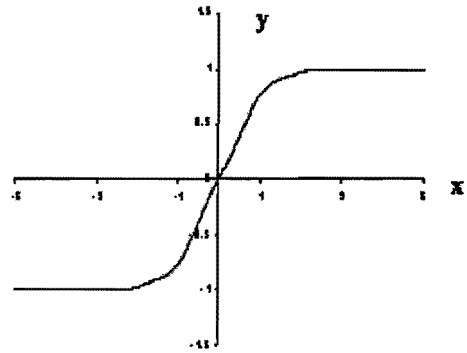

Tan-Sigmoid transfer functio

Figure (3-3): Sample of transfer functions

Note: Matlab provides a variety of transfer function as shown in appendix (A-4).

3-2 The Neural Network Structure

The value of the connection weights in the neural network largely determines the functionality of it. These connection weights can be updated which, in turn results in the network adapting and possibly 'learning'.

Researchers working with neural networks have been inclined to implement a more rigid structure in practice. This is to a degree, due to the abstract nature of the idea. Several simplifications are made:

- The neurons are arranged neatly in layers, either with or without the existence of a connection between two neurons being governed by a strict rule. For example, a common scheme is for the output of each neuron in one layer to be fully connected to the inputs of all neurons in the next. This arrangement is typical of a feed forward network figure (3-4).
- A "learning rule" is defined according to how and when connection weights are updated.
- Connection weights have minimum and maximum strengths.
- All the neurons within a layer, or often the entire network behave in the same way; that is, they all use the same formula to compute an output from the weighted inputs (that depends on the nature of the problem that is presented to the network).

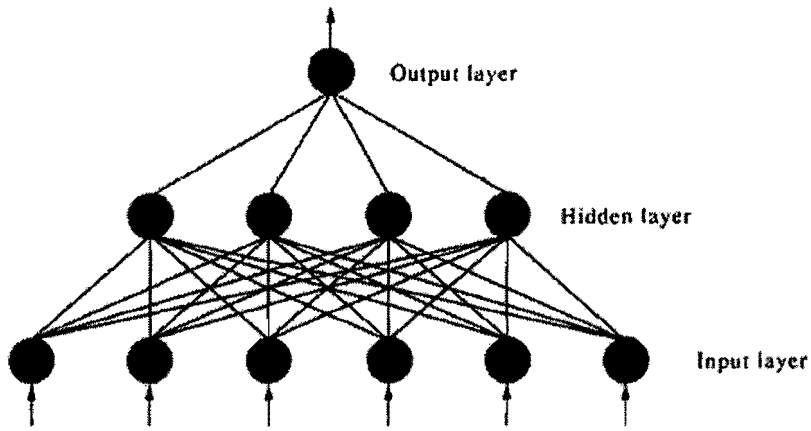

Figure (3-4): A typical feed forward neural network

- Many networks have a further simplification in that they are feed forward networks with no circular information paths; data flows in steps from the input side to the output side. By contrast, recirculation networks do have such circular paths. In this case it is usually assumed that all neurons compute their results simultaneously; these results then map onto a new neural network state, and the process can be repeated.

3-2-1 Neural Network Categories

Neural networks can be categorized according to the type of learning rule employed. (Dougherty 1995) stated that there are three main learning schemes that have been devised, namely; supervised learning, reinforcement learning and self-organisation. Networks, which are not restricted to using one kind of learning, fall into a fourth category and are often called hybrid networks. In this study we will only look at the learning scheme known as 'supervised learning'.

3-2-2 Supervised Learning

In this learning process, an input is presented to one side of a feed forward network, and an output is computed. This is compared with the desired output for these inputs, and a global error function is computed. This is then used to update the weights in order to move the output towards the desired output. Over the course of many examples being presented to the neural network, it is hoped that the global error will gradually decline, as the network converges into a steady state. The learning is described as supervised, because the network is given an exact description of the behavior required after each iteration or epoch. There are many laws (algorithms) used to implement the adaptive feedback required to adjust the weights during training. The most common technique is backward-error propagation, more commonly known as back-propagation.

3-2-3 The Backpropagation Algorithm

The backpropagation algorithm (Rumelhart and McClelland, 1986) is used in layered feed-forward ANNs similar to that shown in figure (3-4). This means that the artificial neurons are organized in layers, and send their signals "forward", and then the errors are propagated backwards figure (3-5). The network receives inputs by neurons in the input layer, and the output of the network is given by the neurons on an output layer. There may be one or more intermediate hidden layers. The backpropagation algorithm uses supervised learning, which means that the algorithm is provided with examples of the

inputs and the desired outputs (this set of the inputs and the desired outputs together, is called the training set), and then the error (difference between desired and expected output) is calculated. The idea of the backpropagation algorithm is to reduce this error, until the ANN learns the training set. The training begins with random weights, and the goal is to adjust them until the error is minimal.

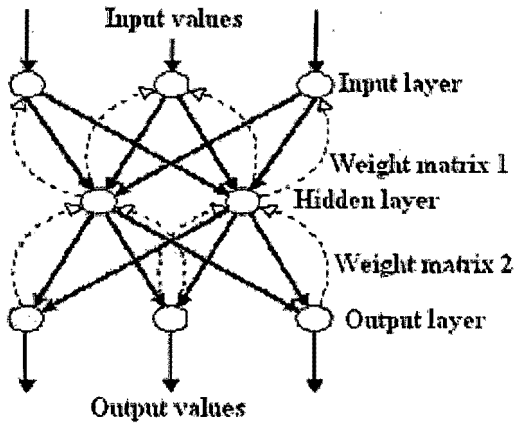

Figure (3-5): Back propogation neural network

3-3 The Basic Mathematics of Back- Error-Propagation

The backpropagation learning algorithm involves a forward-propagation step followed by a backward-propagation step. Both steps are done for each pattern presented during training (Dayhoff 1990).

3-3-1 Forward-Propagation

This step begins with the presentation of an input pattern to the input layer of the network, and continues as activation level calculations propagate forward through the hidden layers. In each successive layer, every neuron (or processing unit) sums its inputs and applies its transfer function (e.g. sigmoid function) to compute its output. The output layer then produces the output of the network.

Figure (3-2) Summarises the specific steps in forward-propagation. Incoming connections to a neuron j are on the left and originate from neurons in the layer below. Output values from these neurons which arrive at neuron j are summed as shown in equation 3.1 above.

Where x_i is the activation level of unit i, and w_{ji} is the weight from unit i to unit j. After the summation function of these neurons are calculated, a sigmoid function is used to compute the output from unit j:

$$f(A_j)=\frac{1}{1+e^{-A_j}} \qquad 3\text{-}3$$

The output from neuron j calculated by the sigmoid function is sent along the output interconnections on the right side of figure (3-2). The same output value is sent along all of the output interconnections.

Notes:

1) The input layer does not perform the weighted sum and sigmoid function calculations. This layer is really only a buffer to hold the input vector. Therefore, it has no weights.
2) Most of the network employs a bias unit in the layer structure figure (3-2). The only difference between this unit and the other input units is in the value of the activation. The activation value of this unit is set to be a constant (usually 1), but the weight value of the bias unit behaves the same as any other weight of the input units.

3-3-2 Backward-Propagation

The back-propagation step begins by comparing the network's output to the target. The error correction step takes place after a pattern is presented at the input layer and the forward-propagation step is complete. Each neuron in the output layer produces an output value, which is compared to the target output that is specified in the training set. Based on

this difference, an error value is calculated for each unit in the output layer. Then the weights are adjusted for all of the interconnections that go into the output layer.

The next step is to calculate the error for all the neurons in the hidden layer that are below the output layer. Then the weights are adjusted for all interconnections that go into the hidden layer. This process continues until the last layer of the weights has been adjusted.

In general, the error value is simple to compute for the output layer and somewhat more complicated for the hidden layers. The error value E_j of neuron j at the output layer is computed as follows:

$$f'(A_j) = (1 - f(A_j))f(A_j) \qquad 3\text{-}4$$

$$E_j = (t_j - a_j)f'(A_j) \qquad 3\text{-}5$$

Where, t_j is the target output of neuron j, a_j is the computed output at neuron j, $f'(A_j)$ is the first-order derivative of the sigmoid function and A_j is the weighted sum of the inputs to j. The value of the ($t_j - a_j$) reflects the actual output error, and the value of $f'(A_j)$ is used to scale this error to force a stronger correction when the sum A_j is near the rapid rise in the sigmoid function curve as shown in figure (3-6).

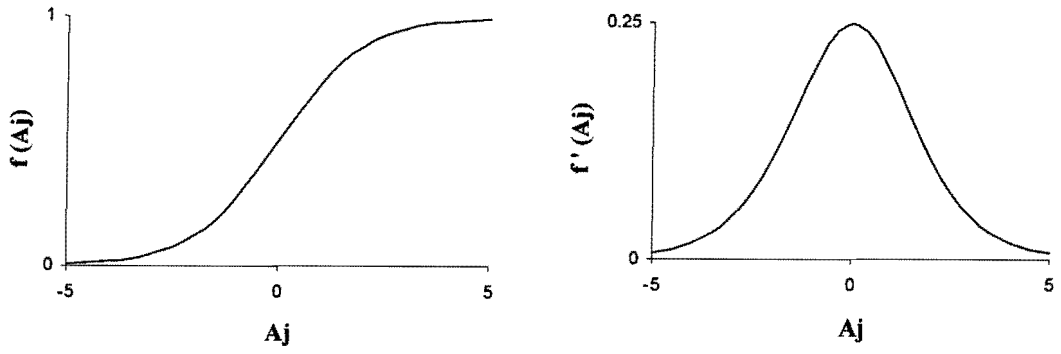

Figure (3-6): The sigmoid function compared to its derivative

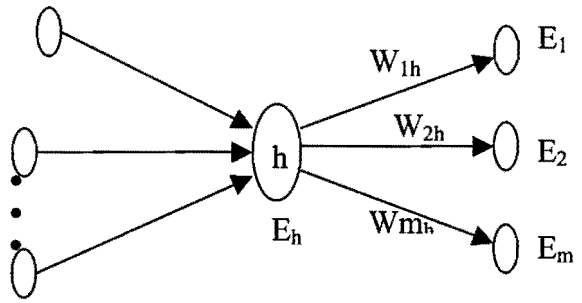

Figure (3-7) : A processing unit in a hidden layer

As shown in figure (3-7) 'h' represents a neuron in a hidden layer. Then the error value of this neuron is calculated as:

$$E_h = \left[\sum_{k=1}^{m} E_k w_{kh}\right] f'(A_h) \qquad 3\text{-}6$$

The first part in this equation is the weight sum, which is taken off the E values of all units that receive output from unit h. The second part is f', it serves to scale the output from unit h by emphasizing the region of rapid rise of the sigmoid function.

By calculating the error, the connection weights can then be adjusted. Each interconnection weight is adjusted by taking into account the value of E of the neuron that receives input from that interconnection figure (3-8). Then the weight can be updated as follows:

$$\Delta w_{ji} = \eta E_j a_i \qquad 3\text{-}7$$

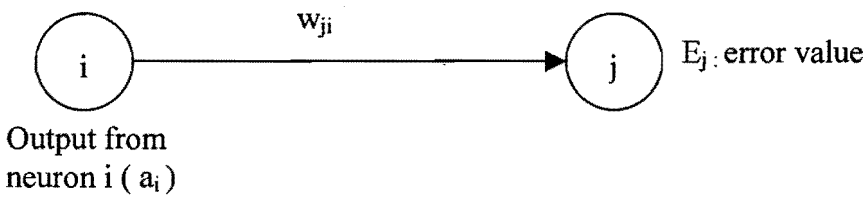

Figure (3-8): Updating a weight

Where w_{ji} is the weight, which goes from neuron i to j. The degree of weight adjustment, depends on three factors. These factors are E_j, a_i and learning rate (η). This weight adjustment equation is known as the generalised delta rule (Rumelhart and McClelland 1986).

3-3-3 The Performance Function

When the network trains successfully, it produces correct answers with increasing frequency as the training session progresses. It is important to have a quantitative measure of learning. One of the performance functions that are used to measure the degree to which learning takes place in the network is the Root-Mean-Squared Error (RMS).

$$RMS = \sqrt{\frac{\sum_P \sum_j (t_{jP} - a_{jP})^2}{n_P n_0}} \qquad 3\text{-}8$$

Where tj_P represents the value for output (i.e. the desired output) after presentation of pattern p, aj_P is the output value produced by output unit j after presentation of pattern p, n_P is the number of patterns in the training set, and n_0 is the number of neurons in the output layer.

This measure reflects how close the network is to getting the correct answers. As the network learns, the RMS error decreases as shown in figure (3-9).

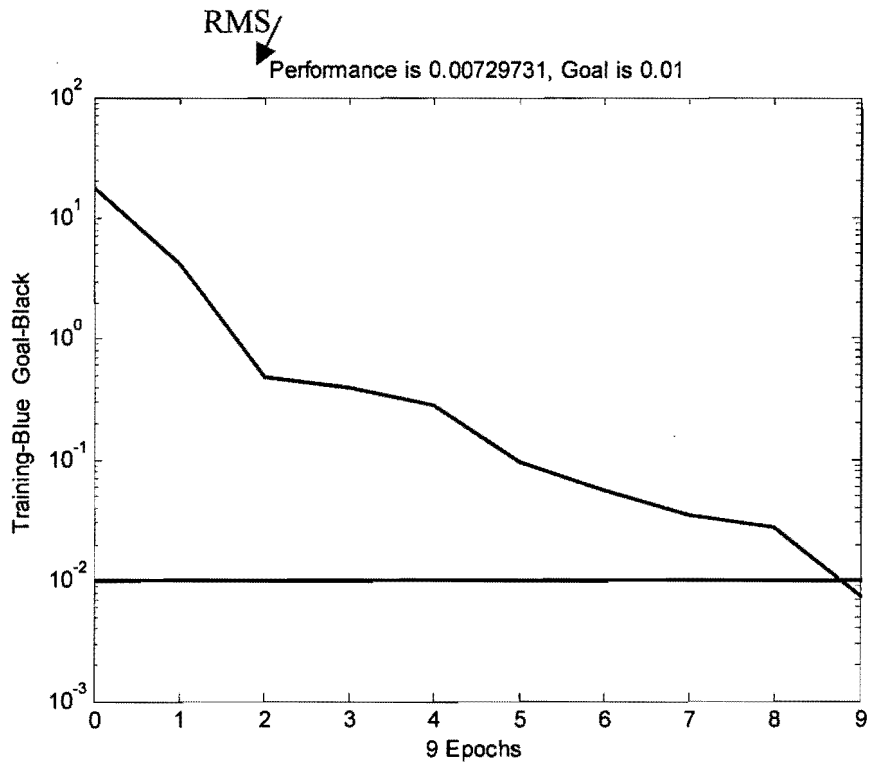

Figure (3-9): Example of the learning curve (From Matlab neural network toolbox)

The parameters of this graph:

Epoch: is the number of iterations during the training

Performance: the performance function of the training in this case is RMS error.

Goal: the minimum error that is required.

Convergence to the correct answer or the goal is not always easy to achieve because the process may take an exceedingly long time and sometimes the network gets stuck in a local minimum and stops learning altogether. To avoid these problems many other training algorithms have been developed since 1986. There are various trade-offs in speed, memory consumption, and accuracy associated with each algorithm.

Matlab provides several variations to the basic training algorithm (back-error-propagation) of the backpropagation neural network, which has been used in this study.

3-4 Training Algorithms

A neural network is not programmed but 'trained'. The algorithm that is used to adjust the weights of the links so as to produce the desired output is known as the training of the network.

There are two different styles of training. In incremental training the weights and biases of the network are updated each time an input is presented to the network. In batch training the weights and biases are only updated after all of the inputs are presented. All the networks that have been trained in this study are based on the batch mode.

The remaining section gives a brief explanation of the different training algorithms that have been applied in this study. For more details about these algorithms, see (MathWorks, Inc 2004).

3-4-1 A Steepest Descent Algorithm

The convergence process of back-error-propagation is basically the same as the gradient descent, which is derived from traditional statistical methodology. However, this algorithm updates the network weights and biases in the direction in which the performance function decreases rapidly; this is the negative of the gradient. This can be represented as:

$$w_{k+1} = w_k - \eta_k g_k \qquad 3\text{-}9$$

Where w_{k+1} is the updated vector of the weight and biases, w_k is a vector of current weights and biases, g_k is the current gradient and η_k is the learning rate. This technique is commonly known as the 'steepest (gradient) descent' neural network training function in which the weights and biases are computed towards the negative gradient of the performance function of the network. The changes to the weights and the biases are obtained by multiplying the learning rate times the negative gradient. The higher the learning rate, the bigger the step is. If the learning rate is set too large the algorithm becomes unstable. If the learning rate is set too small the algorithm will take too long to converge.

The various more advanced versions of the steepest descent algorithm, which exist in Matlab are:

Traingdm: Gradient descent with momentum backpropagation.
Traingda: Gradient descent with adaptive learning rate backpropagation.
Traingdx: Gradient descent with momentum & adaptive learning rate backpropagation.
Trainrp: resilient backpropagation training algorithm.

3-4-2 Conjugate Gradient Algorithm

One of the most often recommended optimization methods to replace the gradient descent is conjugate gradient descent (Masters 1993; Reed and Robert 1999; Bishop 1995), which is a direction set minimization method. Minimization along a direction d brings the function E to a place where its gradient is perpendicular to d. Instead of following the gradient at every step, a set of n directions is constructed which are all conjugate to each other, such that minimization along one of these directions does not spoil the minimization along one of the earlier directions.

The various versions of the conjugate gradient :

Traincgf: Conjugate gradient backpropagation with Fletcher-Reeves updates.
Traincgp: Conjugate gradient backpropagation with Polak-Ribière updates.
Traincgb: Conjugate gradient backpropagation with Powell-Beale restarts.

3-4-3 Newton's method

Gradient methods using second-derivatives (Hessian matrix) of the performance index, such as Newton's method, can be very efficient under certain conditions (Reed and Robert 1999). Where first-order methods use a local linear approximation of the error surface, second-order methods use a quadratic approximation. Because such methods use all the first and second order derivative information in exact form, local convergence properties are excellent. Unfortunately, they are often impractical because explicit calculations of the full Hessian matrix can be very computer resource intensive in large problems.

The various versions of the Newton's method are:

Trainbfg: BFGS quasi-Newton backpropagation.
Trainoss: One step secant backpropagation.

3-4-4 Levenberg-Marquardt

Trainlm: Implements the Levenburg-Marquardt algorithm, which was designed to overcome the problems, associated with having to compute a Hessian matrix. When the performance function has the form of sum of squares as is found in the feed forward networks, the Hessian matrix is approximate as

$$H = J^T J \qquad 3\text{-}10$$

And the gradient is computed as

$$g = J^T e \qquad 3\text{-}11$$

Where J is the Jacobian matrix, which contains the first derivatives of the network errors with respect to the weights and biases, and e is the vector of the network errors.

The Jacobian matrix is calculated through a standard back propagation technique.

Trainlm uses the following formula to update the weight connection:

$$w_{k+1} = w_k - \left[J^T J + \mu I\right]^{-1} J^T e \qquad 3\text{-}12$$

When μ is a scalar that determines how close an approximation is to Newton's method. When μ is zero, then the above function becomes Newton's method. When μ is large, then it becomes gradient descent with a small step size.

3-5 Static Neural Networks

All the networks that have been used in this study are based on the static network. The static network indicates that the network has no feedback or delays. In this case we do not have to be concerned about whether or not the input vectors occur in a particular time sequence, so we can treat the inputs as concurrent. Also, because the input vectors do not interact with one another, their ordering is not important.

3-6 Regression Analysis

The performance of the trained network can be measured by performing a regression analysis between the network response and the corresponding targets. The regression analysis returns three parameters m, b and R. The first two, correspond to the slope and y-intercept of the best linear regression relating targets to the network outputs. A perfect fit matching the targets, would give a slope of 1 and an intercept of 0.

The third value returned by the procedure is the correlation coefficient, R between the targets and the actual network outputs. If the R-value equals 1, then the correlation

between the targets and the outputs is almost perfect. Figure (3-10) illustrates an example of regression analysis.

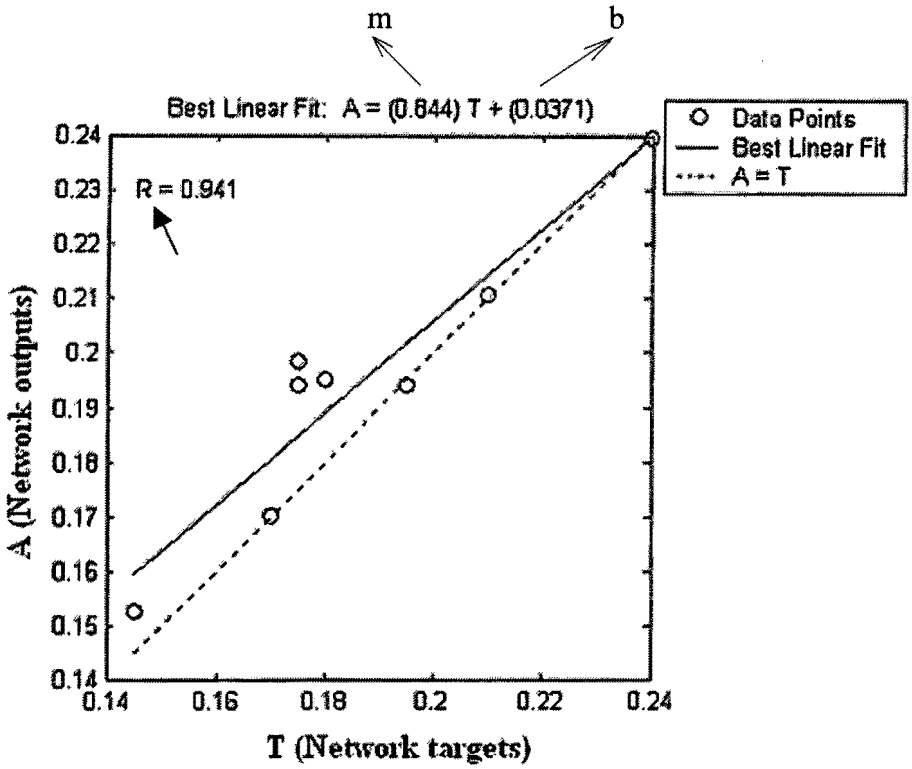

Figure (3-10): An example of regression analysis procedures is automatically carried out using Matlab's function see appendix (A-4).

3-7 The Problems Associated with Backpropagation Training

1- The architecture of a multilayer network is not completely constrained by the problem to be solved.

2- The number of inputs to the network is constrained by the problem and the number of neurons in the output layer is constrained by the number of outputs required by the problem.

3- The type of algorithm of the backpropagation method is crucial, but there is not an optimum algorithm for all situations.

4- The central issue in developing a neural network is generalisation, in other words, how well the network will make predictions for cases that are not in the training

set? NNs, like other flexible non-linear estimation methods such as kernel regression and smoothing splines, can suffer either from underfitting or overfitting. A network that is not sufficiently complex (i.e. few neurons in the hidden layers or no hidden layers at all) can fail to detect fully the signal in a complicated data set, leading to underfitting. A network that is too complex (i.e. having a large number of neurons in the hidden layers or having many hidden layers) may fit the noise, not just the signal, leading to overfitting. Overfitting is especially dangerous because it can easily lead to predictions that are far beyond the range of the training data with many of the common types of NNs.

5- Although there are many rules by which we can compute how many neurons should exist in the hidden layers like the rule of thumb (Masters 1993), these rules are not standard and might not be suitable from one network to another.

3-8 Neural Networks and Umbilical Blood Velocity Waveforms

As previously mentioned, the use of neural networks in the interpretation of blood flow velocity waveforms is not a new technique. Beksac et al. (1995) introduced the first artificial NN system for the evaluation of the umbilical artery. They used a 'supervised artificial neural network' with a Backpropagation learning algorithm. The aim of this system was to decide whether or not the BFVW is normal for a given gestational age, or not. This study was divided into two steps. In the first step automated image processing is initiated after BFVW images are transferred from an ultrasound monitor to a computer. The image processing was then performed on the BFVW for extracting the conventional Doppler indices. They furthermore defined more new indices as illustrated in the previous chapter figure (2-5). The next step was to train the NN with a training set. The input set to the NN was the Doppler indices and the desired output consists of 7 outputs (each representing the normal BFVW's of monthly gestational periods). The network was trained with normal pregnancy only while the testing was performed with both normal and abnormal pregnancy. The specificity and the sensitivity of this system were estimated to be 98.6% and 51.5% respectively. This system was highly specific in predicting normal cases while its sensitivity was relatively poor. Similarly, the positive predictive

value of the abnormal test was poor, primarily because of interpretation problems of umbilical arterial waveforms.

3-9 Summary

The choice of the structure of the neural network is not automatic, but that it depends on the experience and expertise of the designer. An inappropriate structure can yield bad results. At this stage, the choice of the structure is more akin to art than it is to science.

Once the neural network has been structured for a particular application, the network becomes ready to be trained. To start this process the initial weights are chosen randomly. Then, the training or learning process begins. Many methods are available whereby the network 'learns'; however one of these methods has been, adapted in this study, the supervised learning method.

The reason for choosing this method is because in supervised training, both the inputs and the outputs are provided. This set of data, which enables the training, is called the "training set." The network then processes the inputs and compares its resulting outputs against the desired outputs. Errors are then propagated back through the system, causing the system to adjust the weights, which control the network. This process occurs over and over as the weights are continually tweaked. When we have an ANN of hundreds or thousands of neurons, it would be quite complicated to find by hand all the necessary weights. But we can find algorithms, which can adjust the weights of the ANN in order to obtain the desired output from the network. Many algorithms have been developed since the basic training algorithm of the back propagation neural network (back-error-propagation in 1986). Matlab Neural Network Toolbox provides a variety of these algorithms from the slowest ones to the fastest one. In general the gradient descent is very slow because it requires small learning rates for stable learning. The gradient with momentum is usually faster than the standard one, since it allows higher learning rates while maintaining stability. It is also still too slow for many practical applications. If the capacity of the computer is very high it is preferable to use the Levenberg-Marquardt

training algorithm. Should the memory be problematical then a variety of other faster algorithms are available for the large network, for example trainscg and trainrp algorithms. Generally speaking no one algorithm is best for all applications.

Chapter 4. Materials and Methods

This chapter describes how the neural networks are set up and trained using the foetal model in the following steps:

1) First step: In this step we describe the representation of the foetal circulation by a transfer function-based mathematical model in the frequency domain.
2) The second step: The foetal model is generates waveforms at both ends of the cord, which are associated with simulations in which many physiological and anatomical factors are changed in different scenarios.
3) Third step: From the second step we obtain the data that is necessary to train the neural network which is known as the training set. The network is then trained with different types of back propagation algorithms.

4-1 The Foetal Model (developed in a previous project)

There are thousands of physiological factors affecting the shape of the umbilical blood velocity waveforms. Since the effects of the various factors are difficult to investigate clinically, previous work focused on developing a mathematical model of the foetal–placental circulation (Myers 2001, Capper and Myers 2003).

4-1-1 Model Description

The representation of foetal circulation by a transfer function-based mathematical model in the frequency domain was developed to simulate flow waveforms in the umbilical arteries, under both healthy and impaired flow conditions.

The foetal model was based on the arterial dimensions at 28 weeks gestational age (GA). These dimensions have been adapted as follows to take foetal growth into account between 28 weeks and 40 weeks GA.

The typical mass of the foetus vs. GA has been documented. A third-order least-square curve fit was performed on this data to allow the mass to be estimated at any GA. This allows the mass of the foetus, in grams, to be calculated at weekly intervals between 28 and 40 weeks by means of the regression equation (4-1):

$$\text{Foetal mass (GA)} = -0.073GA^3 + 9.95GA^2 - 226GA + 1443 \qquad 4\text{-}1$$

The foetal arterial dimensions at GA between 28 and 40 weeks were calculated by multiplying those at 28 weeks GA by a constant K (size factor), which is equal to the cube root of the ratio of calculated mass, at the required GA, to the mass at 28 weeks (see equation (4-2)). This assumes that the linear dimensions are roughly related to the cube root of the body volume and, therefore, assumes constant density.

$$K = (\text{mass (GA)} / \text{mass(GA=28)})^{\wedge 1/3} \qquad 4\text{-}2$$

The input to the model was a series of current pulses at the foetal heart rate, where current in the model is analogous to volume blood flow in the foetus.

The circulation is divided into short segments; see figure (4-1), so that the dimensions of any arterial segment are less than 10% of the wavelength of the highest frequency component present in the input signal.

Mechanical-electrical analogies are used to represent the mechanical components of each arterial segment by equivalent electrical components, (figure (4-2)).

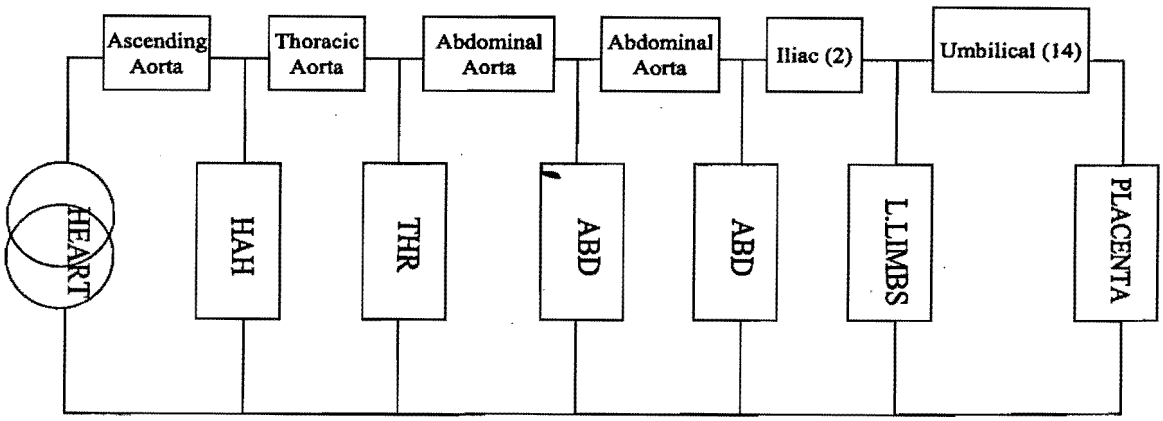

Figure (4-1): Foetal circulation is divided into anatomical regions HAH=head and heart; THR=thorax; ABD abdomen; LEGS=lower limbs; and Placenta. The aorta is subdivided into 4 sections, the iliac arteries into two sections and the umbilical arteries into 14 sections.

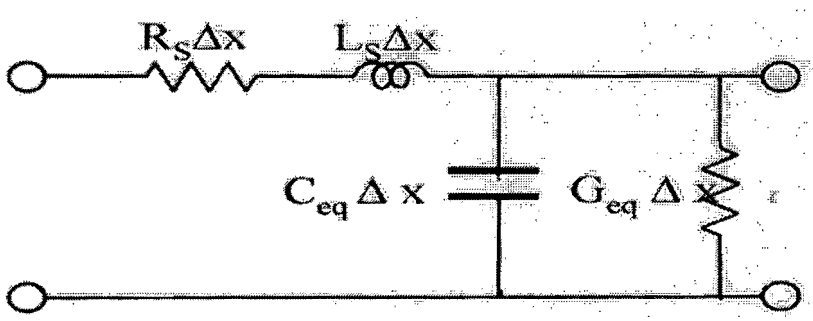

Figure (4-2): Equivalent circuit diagram to represent an arterial segment. R_s and L_s, respectively, represent the resistance and inertance per unit length of the segment due to longitudinal movement of blood in the vessel. C_{eq} and G_{eq} are the equivalent capacitance and conductance per unit length, which represent the effect of a compliant vessel wall.

4-1-2 Representation of the Placenta

The representation of the umbilical placental circulation figure (4-3) is assumed to be:

- Two umbilical arteries are inserted into the placenta, which is assumed to be disk shaped.
- Five chorionic arteries each supply a sector, and 5 branches emanate from each chorionic artery.
- Each of these supplies a vascular tree
- Each vascular tree consists of N large vessels, each branching into M smaller vessels.
- If R_N and C_N and R_M and C_M are the resistance and compliance respectively of the N and M vessels, the impedance of each tree is Zp where:

$$Z_P = \left[\left((R_M / M) // \left(\frac{M}{jwC_M} \right) + R_N \right) \Big/ N \right] // \left(\frac{N}{jwC_N} \right) \qquad 4\text{-}3$$

Where R_N and R_M are the resistance of each of the N large arteries and M small arteries respectively, C_N and C_M are the compliance of each of these vessels, // represents a parallel connection of circuits, and w is the angular frequency.

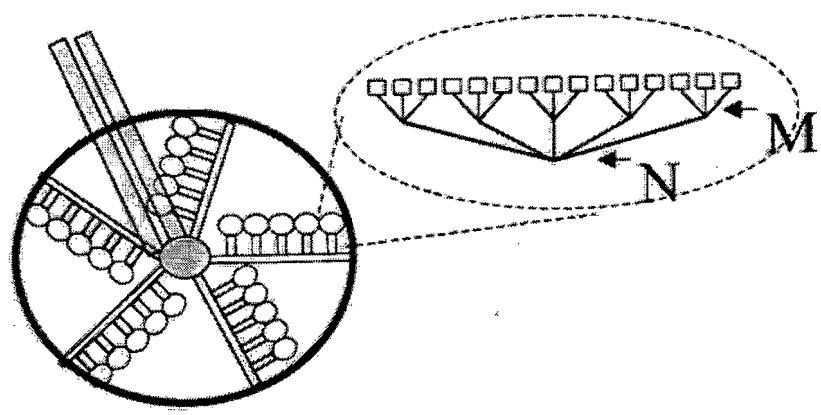

Figure (4-3): The representation of the umbilical placental circulation
N: represents large vessels, M: small vessels.

4-1-3 Blood Flow Distribution

It is assumed that the mean volumetric blood flow from a segment of artery into the vascular bed it supplies is proportional to the mean pressure within the segment and inversely proportional to the resistance of the vascular bed. If v = mean volume blood flow per second to a particular vascular bed and P = mean pressure in the vessel, then the conductance of the vascular bed G= v / P.

Each vascular bed can therefore be represented by a lumped conductive component.
To calculate the conductance of the various vascular beds, it is important to be able to estimate the proportional blood flow distribution in the human foetus.

The cardiac output is assumed to be 500 ml/min/kg of foetal mass. This is distributed to the anatomical regions as shown in table (4-1):

	HAH Head and heart	THR thorax	ABD abdomen	LEG legs	PLA placenta.
Blood flow ml/min/kg	135	75	45	125	120
% Cardiac output	27	15	8	25	25

Table (4-1): Blood flow distribution in the human foetus

4-1-4 Transfer Function Analysis

An equation that describes the relationship between the input pressure (P_{in}) and input flow (Q_{in}) to a particular arterial segment, to the pressure (P_{out}) and flow (Q_{out}) at the output from the segment, can be written as:

$$\begin{bmatrix} P_{in} \\ Q_{in} \end{bmatrix} = \begin{bmatrix} a_{11} & a_{12} \\ a_{21} & a_{22} \end{bmatrix} * \begin{bmatrix} P_{out} \\ -Q_{out} \end{bmatrix} \tag{4-4}$$

It assumed that a matrix could represent each segment of the foetal arterial tree. The individual elements of the matrix are dependent on the properties of the blood, the properties of the arterial wall and the dimensions of the segment.

Hence, all segments from the placenta to the heart are cascaded to form a transfer function that describes the output pressure and flow at the placenta in terms of the input pressure and flow at the heart, as shown in figure (4-4).

Working backwards from the placenta, the pressure and flow calculated here is used to calculate the pressure and flow at the input to any segment along the foetal arterial tree.
By employing this method we are able to calculate the pressure and flow waveforms vs. time along the umbilical artery (14 divisions of umbilical artery).

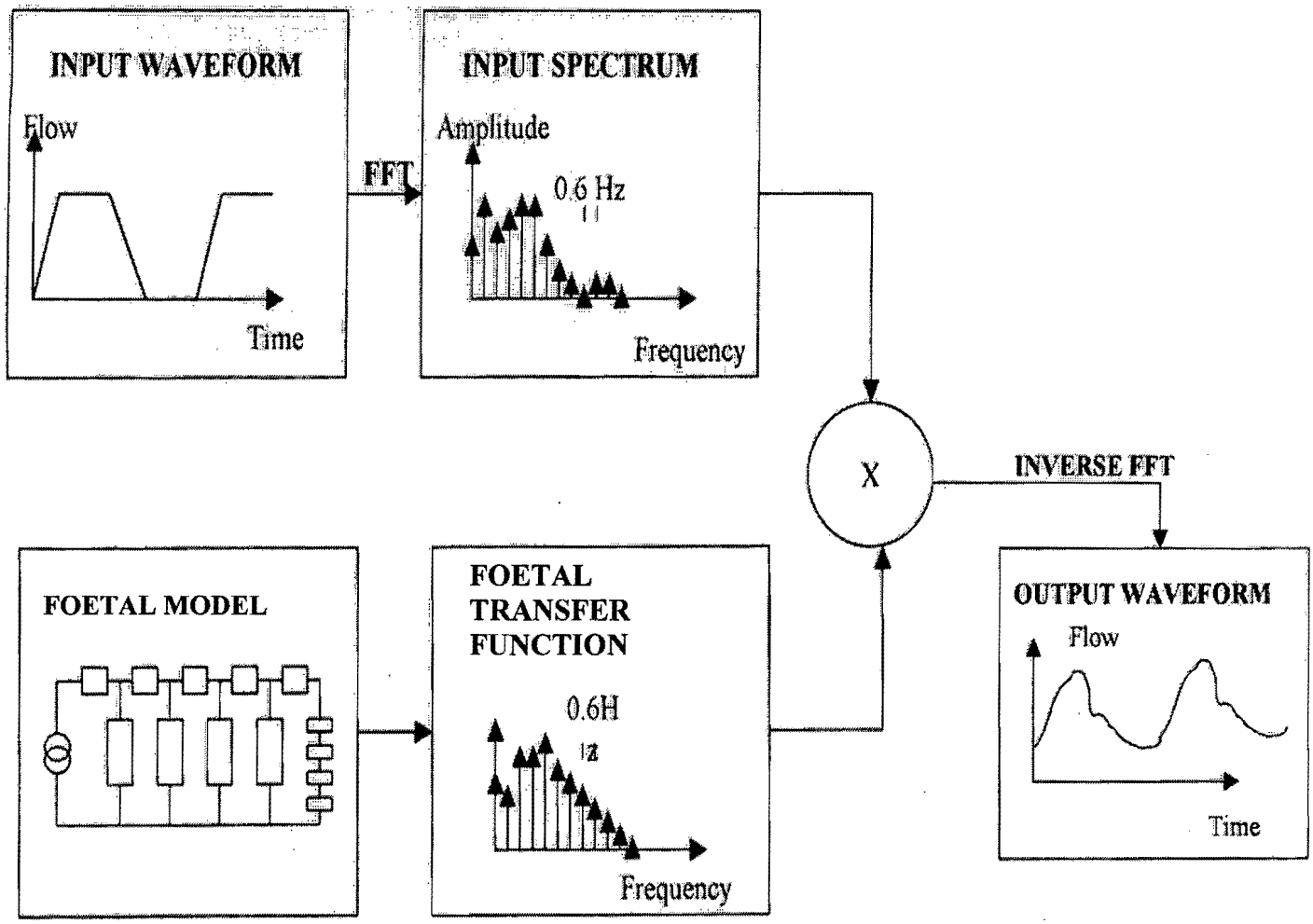

Figure (4-4): Shows an input flow waveform shape that is generated from the heart, each pulse being equal to the stroke volume. This is Fourier transformed to yield the input spectrum. The transfer function of the model is calculated, and this is multiplied by the input spectrum in the frequency domain. The result is inverse Fourier transformed to yield the output flow waveform in the time domain.

4-2 Waveform Generation

The foetal model was used to theoretically investigate the important factors affecting cord flow waveform shape (Myers 2001; Capper and Myers 2003). From the thousands of possible factors, they were able to exclude most as having a negligible effect. However, the most important factors they identified are shown in appendix D.

In the present study, the foetal model suggested by Myers and Capper (2003) is used to simulate umbilical arterial blood flow velocity waveforms at both ends of the cord (i.e. placental insertion and foetal abdominal insertion).

The simulations were performed by varying the physiological and anatomical parameters in the model, each over an appropriate range. Each simulation generates a waveform at both ends of the cord. In all, 2268 simulations were performed, one for each combination of the relevant parameters.

1. Gestational Age: the effects of GA on the umbilical waveforms were simulated in the range 28-40 weeks in steps of 2 weeks.
2. Foetal Heart Rate (FHR): the effect of FHR variations in the range 80 – 180 bpm was simulated in steps of 20 bpm.
3. Umbilical Radius (ur): The effect of the changing umbilical arterial radius in the range 0.1-0.2 cm was simulated in steps of 0.02cm.
4. Placental Simulation: We simulated the placenta in different scenarios as follows:
   4.1 A foetus with normal placental resistance: When the dimensions of all arteries are assumed to be normal for each gestational age; the flow distribution assumed for a normal foetus is 25% of the cardiac output distributed to the placenta, 27% to the head and heart, 15% to the thorax, 8% to the abdomen and 25% to the lower limbs.
   4.2 A foetus with increasing placental resistance: The percentage blood flow to the placenta was decreased in steps from the normal value (25% of CO) to different values. This was done by decreasing the number of small arteries in

the placenta (i.e. this is accomplished by decreasing M and N). This simulates either obliteration of the small arteries of the placenta, as has been reported by (Giles et al. 1985), who performed a histological examination of the placenta in patients with abnormally high index values, or mal-development of the villous tree, as reported by Krebs et al. (1996). In this simulation, blood flow to the head and heart of the foetus was augmented in proportion to the decrease in flow to the placenta.

4.3 A foetus with decreased placental resistance: Here the percentage blood flow to the placenta was increased in small steps by increasing the number of small arteries in the placenta (i.e. increasing M and N).

5. Umbilical length (ul): Because the umbilical arterial length is more difficult to quantify in vivo, the cord length was simulated as growing normally with gestational age.

4-2-1 Summary of the Simulation Process

Each time one of the aforementioned physiological or anatomical factors of the foeto-placental circulation was changed, other factors remained constant. In this simulation we have taken into account all probabilities in foetal health or foetal disease that could be associated with the foetus, as shown in table (4-2).

The variable	n:(iteration number)	Step size	Starting dimension	End dimension
GA	7	2	28	40
Ur	6	.02	.1	.2
FHR	6	20	80	180
N	9	2	4	20
The total number of umbilical waveforms = 7*6*6*9 = 2268 waveforms				

Table (4-2): Summary of the simulations using the foetal model

Where:

GA : gestational age in weeks

ur : cord radius (cm)

FHR : foetal heart rate (bpm)

N: the number of large vessels within the placenta

n: the iteration number for each variable ,

= ((end dimension -starting dimension)+step size)/ step size

4-3 Back Propagation Neural Network Methods

Most of the medical diagnoses, either for prediction or pattern recognition employ back propagation neural networks. Because these types of neural network have achieved good results, we have chosen the same algorithm to begin our training of the neural network. Furthermore, there are many variations of the back propagation algorithm, we therefore tested our data with several types of algorithms.

The architecture that is most commonly used in the back propagation algorithm is the multilayer feed forward network. In the multilayer network there is an input layer, an output layer and one or more hidden layers. In Matlab convention, the input layer is usually not counted when counting the number of layers of a neural network.

4-3-1 Procedures

Several neural networks were designed, created, trained and evaluated in an effort to find the appropriate neural network architecture and training method for use in the foetal model data.

4-3-2 Creation

Creating a neural network is simply a matter of calling the appropriate Matlab function and supplying it with the necessary information. For example, the following code creates a new feed-forward network that uses the hyperbolic tangent sigmoid transfer function (tansig function) in the hidden layer, while the transfer function for the neurons in the output layer is a linear transfer function (purelin function). The network is then trained with Levenberg-Marquardt backpropagation.

net = newff(mm, [20 3], {'tansig' 'purelin'}, 'trainlm'} 4-5

This network has an input layer (accommodate the input vector), a hidden layer consisting of 20 neurons, and an output layer consisting of 3 neurons. mm is a matrix of size number of inputs x 2. Each row contains the minimum and maximum value that a particular input can have (see appendix A-4 for more details).

4-3-3 Neural network Training

Neural networks are good pattern recognition engines because they can often generalize and correctly classify inputs they have not previously been seen. In order to generalise; large amounts of data should be used during the training process. Therefore, the foetal model allows us to generate thousands of waveforms to train the neural network. These data obtained from the foetal model are used as a training set for the neural network.

Training set: is a collection of the input set and the desired output set that are used to train the network.

4-3-4 Training Set of the Neural Network

Each of the simulations performed in step 4-2 resulted in the generation of a waveform at each end of the umbilical cord. These waveforms were then used to calculate indices at each end of the cord for each simulation, namely RI_p, PI_F,PI_P and PI_F.

where,

RI_P, PI_P = resistance index and pulsatility index respectively at the placental side.
RI_F, PI_F = resistance index and pulsatility index respectively at the foetal side.
These variables, together with FHR and GA, are used as input set to the neural network.
The variables of the input set to the neural network are:
(RI_P , PI_P , RI_F , PI_F , FHR , GA)
The variables of the desired output set from the neural network are:
ur , ul , N

4-3-5 Neural Network Architecture and Network Parameters

As yet there is no theory to tell us how many neurons in the hidden layers are needed to approximate any given function. Therefore, two different networks are created, one with one hidden layer and the second with two hidden layers. The hidden layer size is initially set to 20 neurons for the network with a single hidden layer and to 20 each for the network with two hidden layers. The performance goal of the network between the desired output and the actual network output are set to 1e-2. The transfer functions that are used are the tansig function for the hidden layers and the purelin function for the output layer see appendix (A-4).

The following table (4-3), summarises the initial parameters that set all the neural networks with one hidden layer and with two hidden layers:

	Number of layers	Max Epochs	Performance goal	Number of neurons in the hidden layers
First network With 1 HL	2	500	1e-2	20
Second network With 2 HL	3	500	1e-2	20 - 20

Table (4-3): Network Parameters

Notes for table (4-3):

HL = hidden layer

Again the input layer is not counted when counting the number of layers of a neural network.

2 = one hidden layer and one output layer

3 = two hidden layers and one output layer

4-3-6 Evaluation of the network

The performance of the trained neural network can be measured by carrying out regression analysis between the network response and the corresponding targets.

The network has three output factors, namely ur, ul and N. The trained network's performance can be determined with any of these factors, however we chose to measure the performance of the trained network with the umbilical radius ur only. The reason is because clinically we could only measure the umbilical radius with Doppler equipment, and we were unable to determine ul or N.

4-4 Clinical Data

One of the problems that occurs during neural network training is called overfitting. The error on the training set is driven to a very small value, but when new data is presented to the network the error is large. The network has memorized the training examples, but it

has not learned to generalize to new situations. The best way to avoid overfitting is to use lots of training data. We need the neural network to generalise well, not only with the foetal model data but also with the clinical data, so simply generating more data from the foetal model is not sufficient. Therefore it was necessary to use clinical data in a way to measure the ability of the trained neural network performance on unseen data.

In the clinical trial, 29 pregnant women were studied, of these 10 were normal while the remaining 19 had pathology associated with pre-eclampsia and hypertension. The gestational ages of the foetuses were chosen to match the foetal model. This was in the range between 28 to 40 weeks. The studies were performed with Colour -Flow Ultrasound equipment.

Note: 3 pregnant women of 29 were excluded from further analysis in the next chapter, for reasons that will be described in chapter 6.

4-4-1 Doppler Measurements

The umbilical cord was visualized with colour-flow ultrasound, and both the placental and foetal abdominal insertions were identified. Measurements of Doppler indices namely, the resistance index (RI) and pulstality index (PI) were calculated at both ends of the umbilical cord. The foetal heart rate as well as the umbilical radius was measured using the same Doppler equipment.

A sonographer from Tygerberg Hospital, South Africa performed the measurements on a weekly basis and provided us with data (4 cases every week).

4-5 Generating of Centiles

This step was performed in order to gain a deeper understanding of the foetal condition. The trained neural network predicts the physiological patterns that are associated with umbilical waveform using different combinations of ur ,ul and N. As far as we know the

only centiles graphs available are for RI and PI with GA. These graphs make it possible for clinicians to gauge normality and abnormality of RI and PI at any GA. As a result the foetal condition can be evaluated. The aim of this step is to plot centiles for ur and N with the gestational age.

4-6 Consideration of the Location of Doppler Measurements along the Umbilical Cord

Other serious issues that render Doppler ultrasound a poor tool in foetal medicine were explained in section 2-3-2. The main issue here was the location of measurements along the umbilical cord. As far as we know from the literature, no satisfactory or exact explanation for this issue exists. The result of this issue is that some hospitals do the measurements at the foetal side, others at the placental side.

The big question however is, whether there is enough information about the measurements taken from one location along the umbilical artery for decision making about the foetal condition.

Chapter 5. Results

This chapter describes how the neural networks are tested using clinical data, and analysis the results from the trained neural networks, in the following steps:

1) The First step: The problem of generalisation is a significant issue in any neural network application. In an attempt to solve it, a sample of 26 pregnant women is chosen for testing the performance of the trained neural network.
2) Second step: Here the predicted values from the neural network which represent the anatomical and the physiological factors that are associated with each clinical waveform, will be interpreted by creating two centile graphs.
3) Third step: The location of the measurements of Doppler ultrasound along the cord will be taken into consideration.

5-1 The Results Obtained From Training The Neural Network

Many variations of back propagation algorithms are provided by Matlab NN toolbox see appendix A-4. The performance (based on the regression coefficient of predicted versus actual radius) of the tested multilayer feed forward neural networks with back propagation, are summarized in the following table:

Algorithm	R1 – 1 HL	R2 – 2 HL
Traincgf	.816	.643
Traincgp	.66	.872
Trainrp	.923	.928
Traingdm	Inf	.14
Trainoss	.626	.603
Trainbfg	-.0866	-.188
Traingda	.189	.486
Traingdx	.0878	.0843
Trainscg	.84	.673
Traincgb	.847	.641
Trainlm	.982	.988

Table (5-1): The performance, as measured using the correlation coefficient R of different training algorithms (based on foetal model data).

Note that R is a measure of the correlation between the true value of ur and the value of ur predicted by the neural network. The highlighted boxes denote the best algorithms based on their high correlation coefficient (R>0.9).

5-1-1 Refining the Neural Network Using Clinical Data

We observe from table (5-1) that only 2 algorithms behaved successfully, namely trainlm and trainrp. These algorithms have correlation coefficients >0.9.

Up to this point, the neural networks have been trained only with data that was generated by the foetal model. Because we need the neural network to quantify patterns with real clinical data, 26 pregnant women were chosen, on whom the trained neural networks with algorithms trainlm and trainrp for one and two hidden layers were tested.

5-1-2 The Training Methods

1) The parameters of network 1 (trainlm algorithm) and network 2 (trainrp algorithm) are shown in table (5-2).

The parameters of network 1 and 2 with different neurons in the hidden layers					
	Number of layers	Max Epochs	Performance goal		Number of neurons in the hidden layers are
Network 1 (trainlm)	2 and 3	50	1e-2	After training & testing	8 for 1 HL 6 , 6 for 2 HL
Network 2 (trainrp)	2 and 3	3000	1e-2		50 for 1 HL 25 , 25 for 2 HL

Table (5-2): Network Parameters

2) Creating several networks for each network 1 and 2 with different neurons in the hidden layers.
3) The training set; input set and the desired output set for each neural networks are the same as described in section 4-3-4, namely those generated using the foetal model. Then all the networks are trained to meet the goal 1e-2.
4) When the networks trained successfully the trained neural network is now ready to test on a new data set not yet seen by the networks.
5) The new data set consists of 26 patients' clinical data. In each case the input is (RI_P, PI_P , RI_F, PI_F , FHR, GA). This new input set will be simulated with each trained neural network. The results from the simulation produce three factors (cord radius, cord length and the number of large vessels N). These are known as the actual network output of the trained neural network. To measure the performance of the networks we need the desired output set. The only parameter available from the clinical data, as a desired output, was the umbilical radius,

which was measured by the Doppler equipment. Therefore, the performance of the trained neural network between, the radius that was measured clinically and the radius that was predicted from the networks, was measured using regression analysis.

6) By measuring the performance of all trained networks, then we choose the networks that produce the best correlation coefficient with the clinical data 26.
7) The final number of the neurons for each hidden layers for both network 1 and network 2 are shown in the highlighted column of table (5-2).

The following graphs show the performance of the chosen trained neural networks using the regression analysis based on the clinical data (26 cases):

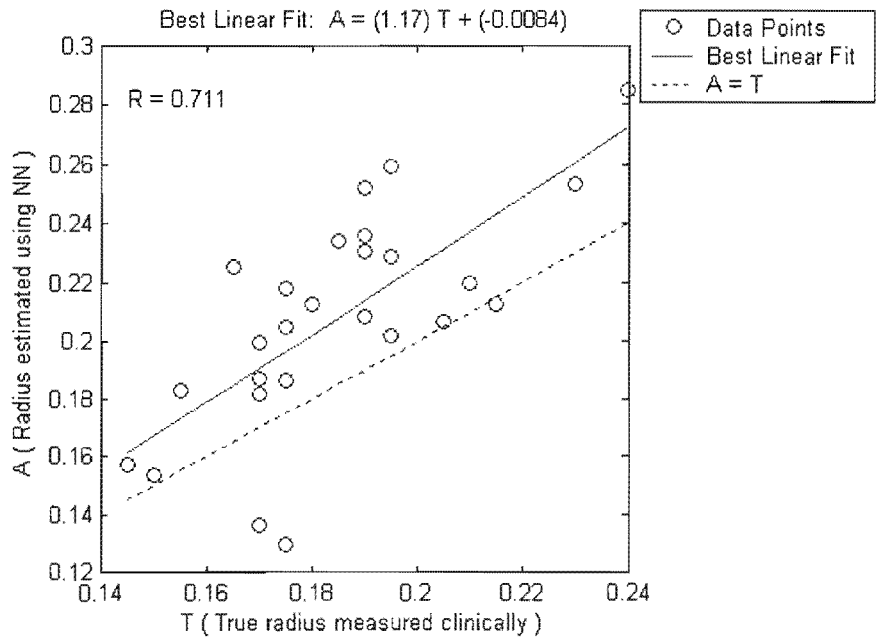

Figure (5-1): Shows regression analysis with trainlm algorithm for one hidden layer

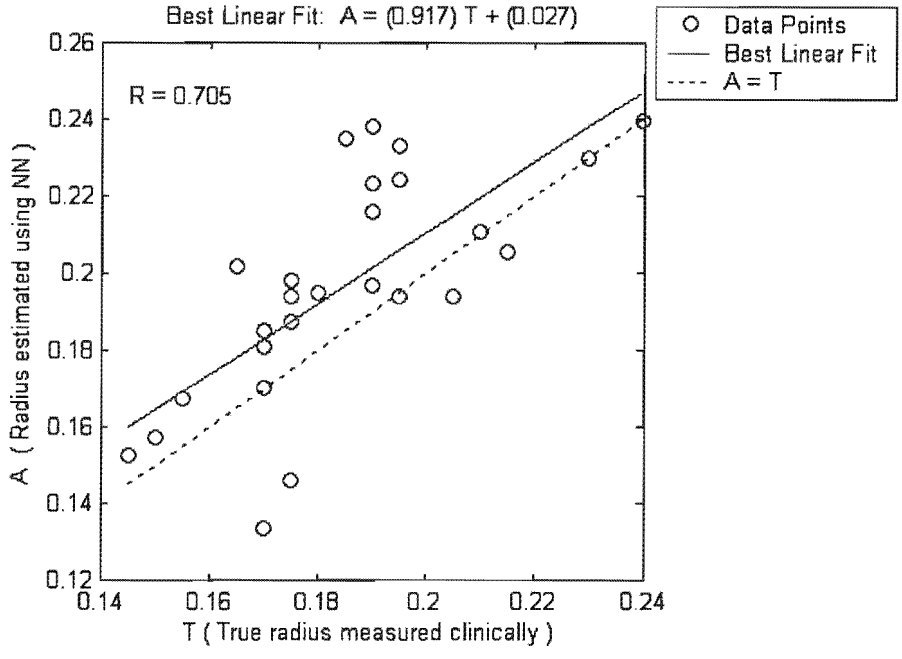

Figure (5-2): Shows regression analysis with trainlm for two hidden layers

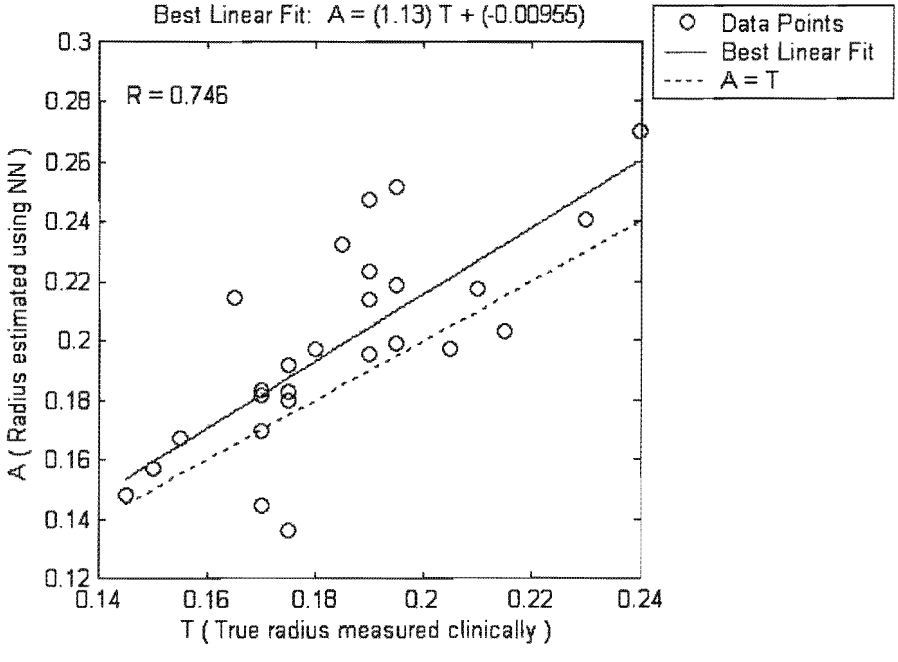

Figure (5-3): Shows the regression analysis with trainrp for one hidden layer

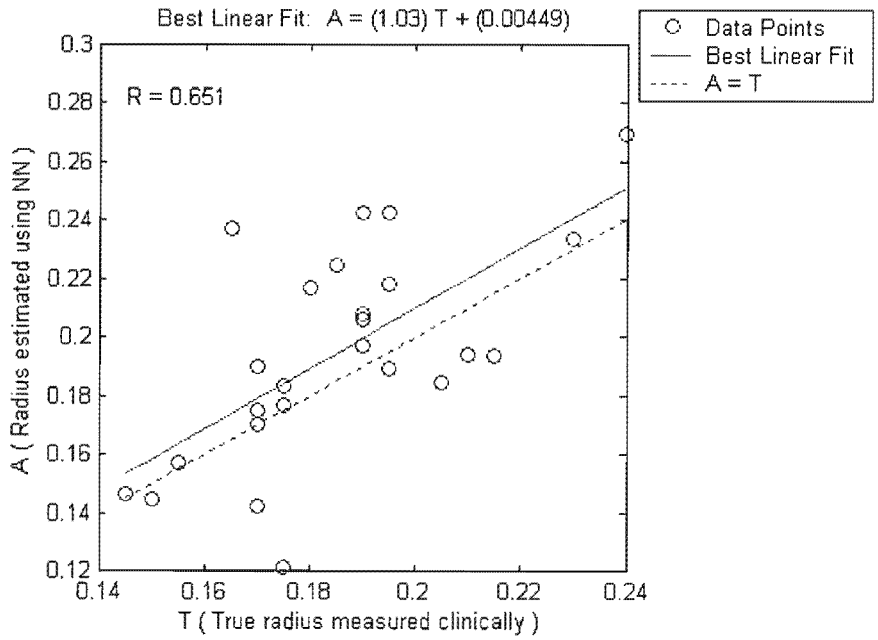

Figure (5-4): Shows regression analysis with trainrp for two hidden layers

The data results of simulation of the chosen trained networks either with trainlm or trainrp algorithms, with one or two hidden layers based on the clinical data of 26 pregnant women are shown in tables (E-1,E-2) of appendix E.

5-2 Results of the Second Step (Generating the Centiles)

The physiological and anatomical patterns associated with clinical data waveforms are not known. These patterns have been predicted using the trained neural networks 1 and 2. These patterns for cord radius and N are shown in tables (E-1, E-2) of appendix E.

The hospital only provided us with the health status of the pregnant women, at the time that the measurements were taken. These measurements were either normal or abnormal. Moreover, they supplied us with the umbilical waveforms, through which the Doppler indices were obtained; these were used as an indicator for foetal health.

Although some women were suffering from pre-eclampsia or hypertension the Doppler indices were normal. Because of this contradiction some assumptions had to be made, in an attempt to interpret these patterns for better evaluation of the foetal condition.

5-2-1 Assumptions

The foetal model is a simulation of foeto-placental circulation. It is possible to generate thousands of umbilical arterial waveforms by changing the physiological patterns in the foetal model. To achieve this clinically is quite difficult.

We could create new graphs (centiles) for these patterns to reveal how they behave with Doppler waveforms at each gestational age. This is done as follows:
Section 2-4-1 described that many groups have published a reference range for normal pregnancy for RI vs. GA. One of these reference ranges was generated by Tygerberg Hospital (reference range for RI vs GA) as shown in figure (5-5). We used this group as a reference for this task.

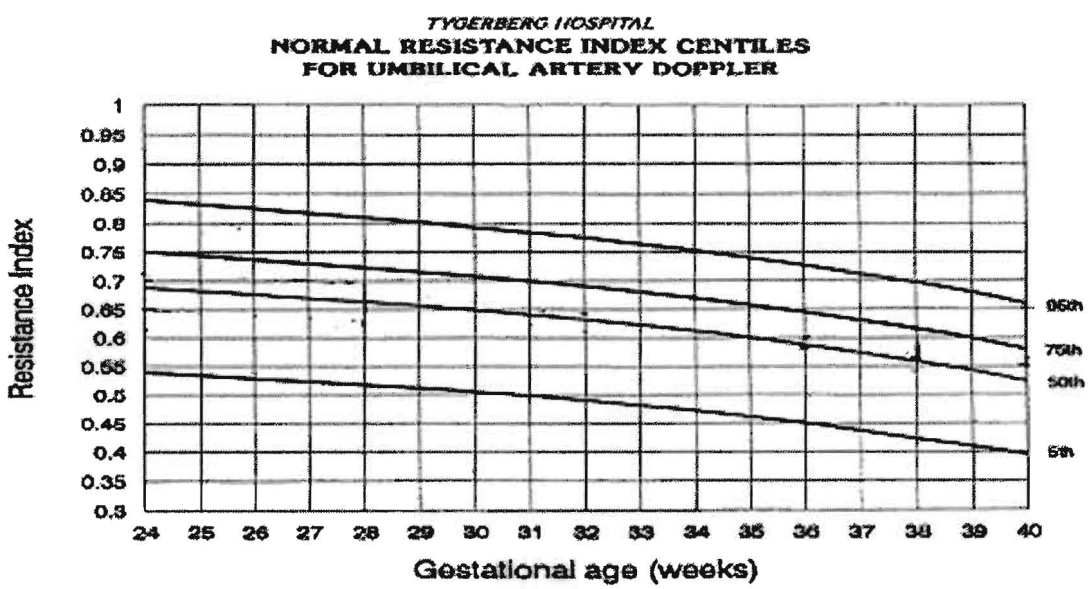

Figure (5-5): Normal resistance index centiles for the umbilical artery from Tygerberg Hospital-South Africa.

The normal range of RI was limited, by this graph, for each gestational age. This information was used as a filter.

Note: The RI vs. GA graph is used by Tygerberg hospital to investigate the value of the RI only at the foetal abdominal insertion site, although this graph was constructed based on continuous Doppler equipment. Therefore, we intend to use this graph to investigate the values of RI at the foetal side as the hospital does.

5-2-2 Creating The Centiles For The Number Of Large Vessels N And The Umbilical Diameter Vs. GA

The foetal model was simulated by changing N in different scenarios from low to large values at each gestational age, keeping the other parameters constant, at their normal value. The results from this simulation are that the percentage blood flow to the placenta changes. The physiological and anatomical parameters used in each simulation are recorded, together with the Doppler indices generated at each end of the cord. The Doppler indices undergo a filtering with the normal range for RI described earlier. This generates the normal range for N. By plotting N vs, GA we get the centiles graphs for N vs GA figure (5-6).

The same procedure was performed with the umbilical radius. Here we assumed that the umbilical arterial radius undergoes changes in different scenarios at each gestational age from 28 to 40 weeks, keeping the other factors constant. By plotting umbilical diameter vs, GA we get the centiles graphs for the umbilical diameter vs GA figure (5-7).

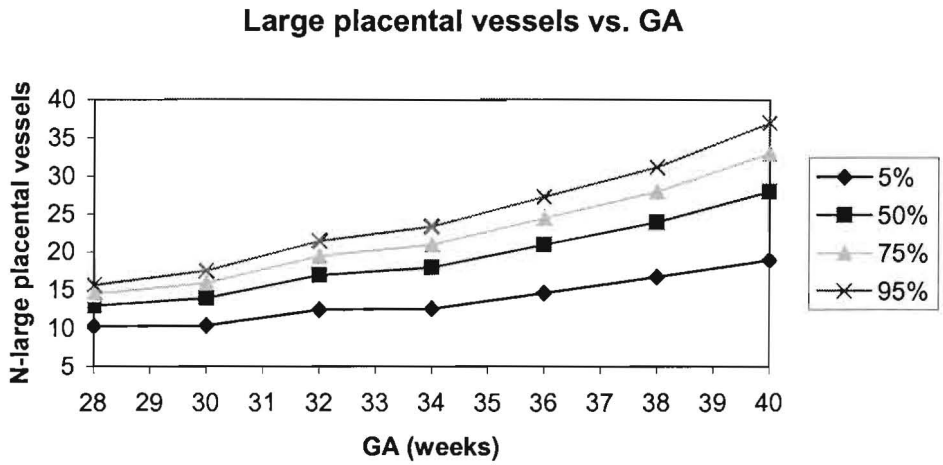

Figure (5-6): Centiles for the number of large vessels (N) within the placenta vs. GA generated by the foetal model.

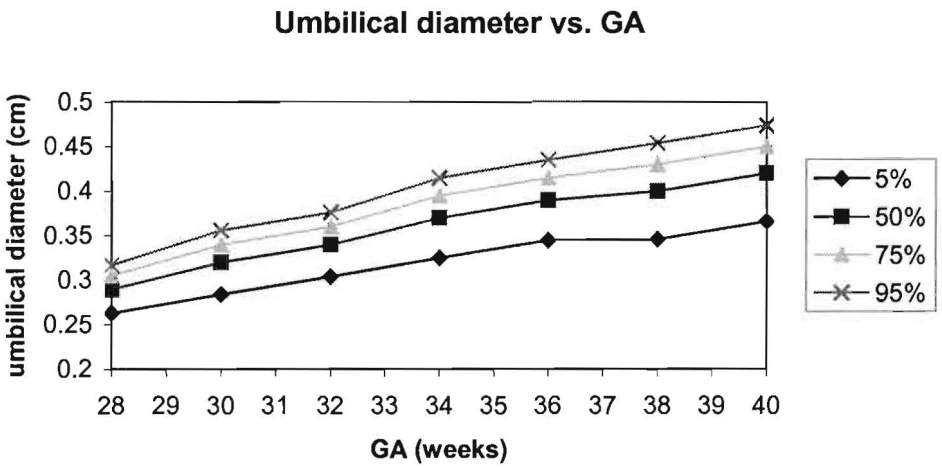

Figure (5-7): Centiles of umbilical diameter vs. GA generated by the foetal model.

5-3 The result of Location of Measurements along the Umbilical Cord

Our explanation of the issue of site of measurement in the cord is that there is not enough information for clinical decisions to be made from one location. Two methods were used to prove this.

5-3-1 Method 1: Two Locations Methods

Training neural networks from one location (either the foetal or placental end) was impossible see figures (5-8, 5-9). Here the simulation was terminated unsuccessfully after 4000 epochs. This reflects that there is not enough information available when using one location of the cord. It is therefore necessary to use two locations. The result of using two locations is that the network trained in less than 15 epochs Figure (5-10). Because it is possible to visualize the placental and abdominal insertion sites using Doppler equipment, we decided to use the ends of the cord for waveform acquisition.

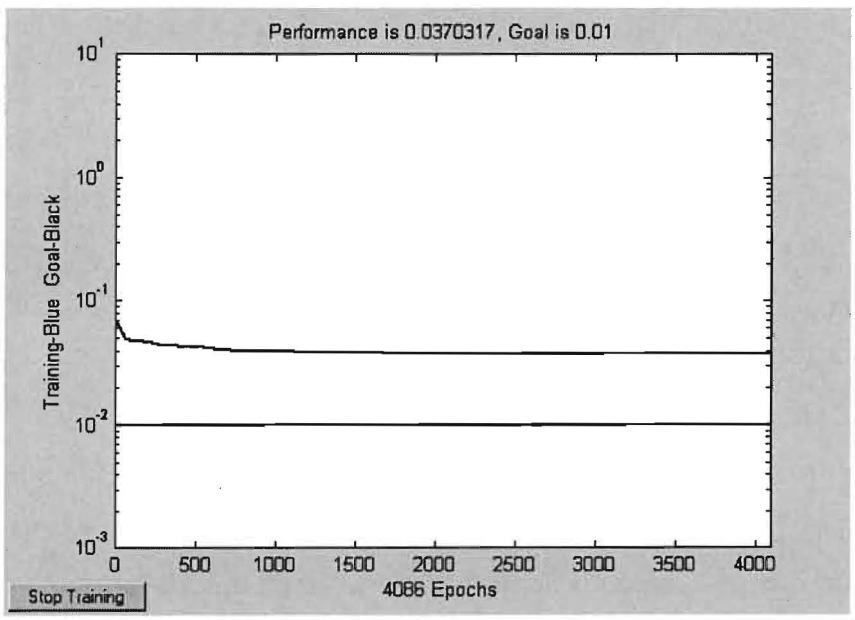

Figure (5-8): Attempted training of the NN with the trainlm algorithm and with two hidden layers using only the placental insertion side of the cord

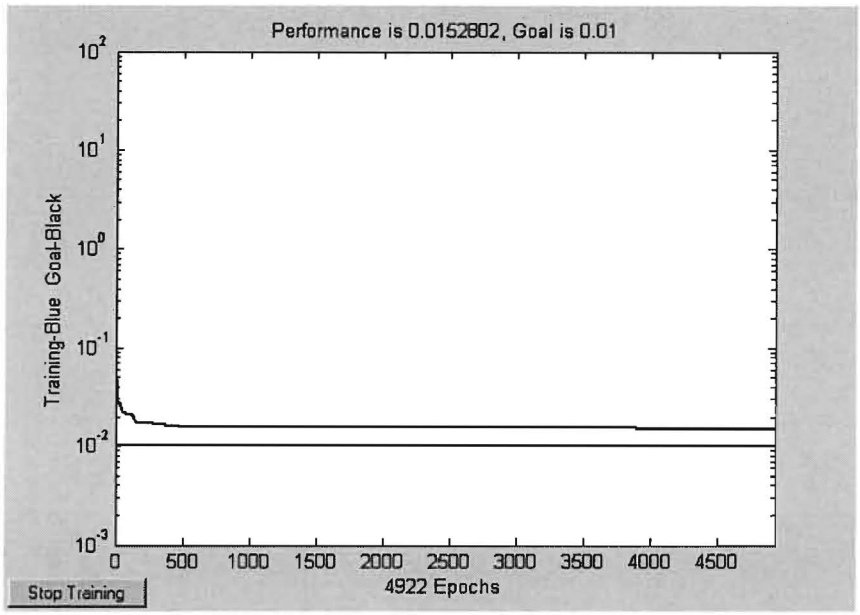

Figure (5-9): Attempted training of the NN with the trainlm algorithm and with two hidden layers using only the abdominal insertion side of the cord.

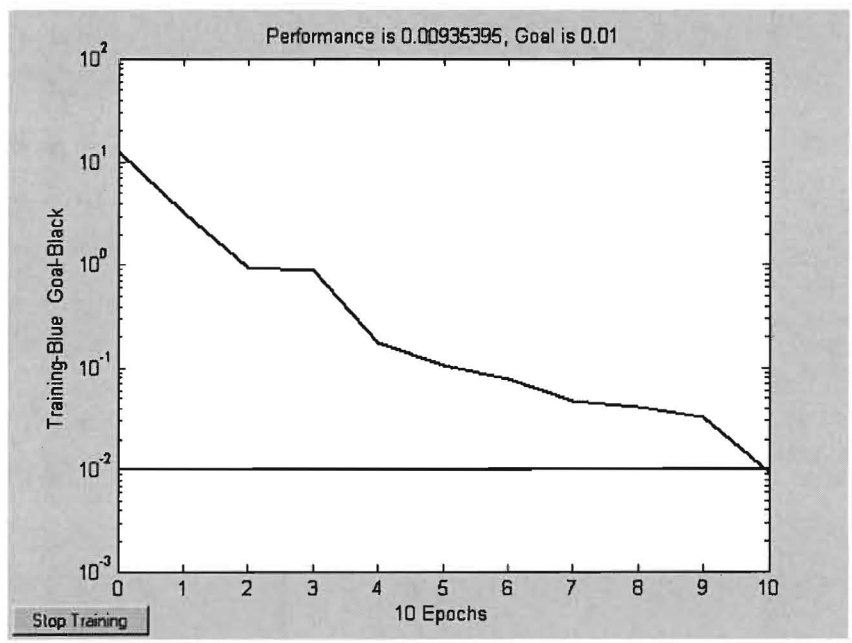

Figure (5-10) : Training the NN with the trainlm algorithm and with two hidden layers for both ends of the cord; the placental side and the foetal abdominal side.

5-3-2 Method 2: Reflection Coefficient Method

As previously mentioned, training neural networks based on one location was impossible. The measurements from one location could be improved either by using a second measurement site or by using the reflection coefficient RC see appendix B. We proved in section (5-3-1) that training neural networks using both locations of the cord was very successful and the training took just a few epochs to converge to the solution.

We are now going to prove the other way of solving this problem using one location of the cord and adding a new factor, " the reflection coefficient" and testing whether the networks converge and train successfully.

The Training Methods

The parameters of the network that are used here are as follows:
The structure of the network that is used is a multilayer feed forward neural network with one hidden layer. The number of neurons in the hidden layer is 15 and the training algorithm is trainlm.
The foetal model runs in the same way as the simulation that was shown in table (4-2). The extra calculation included in this simulation is that a new factor (the reflection coefficient) was calculated for each simulation.
RC = (Placental impedance – Characteristic impedance) / (Placental impedance + Characteristic impedance).
The input to the network was the same input set that was used for section (4-3-4). In that section we used both locations as input to the neural network but here we used each location separately; either the placental side or the foetal side.
The input for the placental side is (RI_P, PI_P, FHR, GA + RC) and the foetal side was (RI_F, PI_F, FHR, GA + RC). Both locations were trained separately. The desired output of the neural network for each location was the same as that used in section (4-3-4) and they are (ur, ul, N).
Training both networks are shown in the following figures (5-11, 5-12)

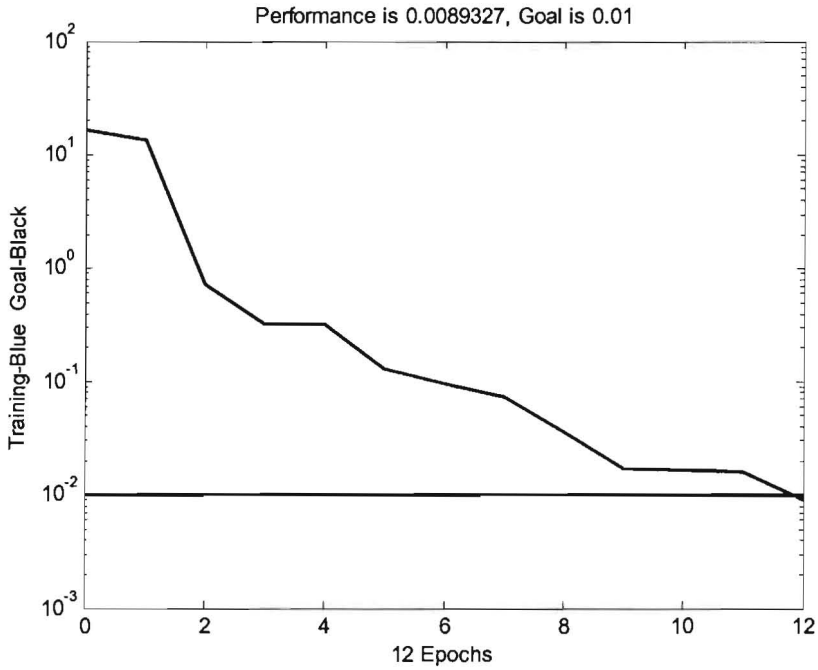

Figure (5-11): Training the network based on one location, the placental side, using the reflection Coefficient.

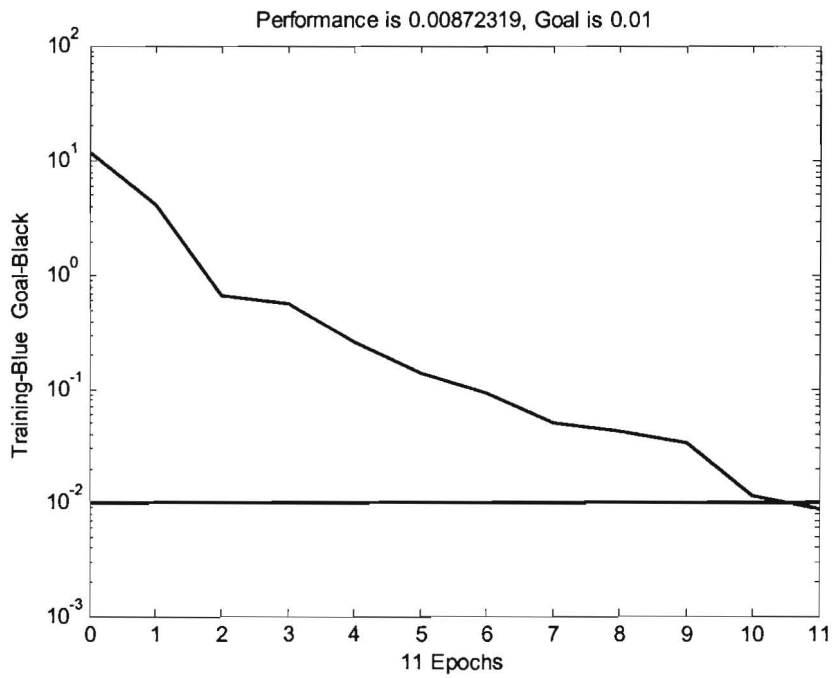

Figure (5-12): Training network based on one location, the foetal side, using the reflection coefficient.

The following table (5-3) summarizes the capabilities of differently trained networks based on different locations, using the reflection coefficient as input or without using this coefficient.

The Input to the neural network	Epochs	Time	Convergence Goal = 0.01
Abdominal side without reflection coefficient	4922	6 hours	0.0152
Placental side without reflection coefficient	4086	8 hours	0.037
Abdominal side using reflection coefficient	11	72 seconds	0.0087
Placental side using reflection coefficient	12	91 seconds	0.0089

Table (5-3): The Comparison between different networks based on one location Adding the Reflection Coefficient or not.

5-4 Training the Network Using both the Doppler Indices and the Umbilical Radius.

Because we can clinically measure the umbilical radius with ultrasound equipment, we have studied the effect of using the umbilical radius as input to the neural network instead of as an output. In other words, we want to study the effect of using Doppler indices from both locations on the cord, as well as using the radius as an input .

We used the multilayer feed forward neural network with the trainrp algorithm with one hidden layer.

The training set would be the same as used in section 4-3-4. The umbilical radius, however, would be used as input in this case, while the output set would be cord length ul and N.

The parameters of the network using the trainrp algorithm with one hidden layer are as follows:
Numbers of neurons in the hidden layers = 50.
Maximum training epochs =900
Performance goal = 1e-2
The transfer function of the hidden layer was the tansig function and for the output layer it was the purelin function.

5-4-1 Training Method

Firstly, the neural network was trained using the foetal model data using radius as input. Then the trained neural network was used to predict ul and N for the clinical data set of 26 patients.

The values for N generated using this method were plotted against those generated previously (without using ur as an input). This is illustrated in the fourth column of table (E-1) of appendix E. The correlation between these two N's was calculated, as illustrated in figure (5-13).

The data results from the simulation of both networks with trainrp using the radius as input and output is illustrated in table (E-3) of appendix E.

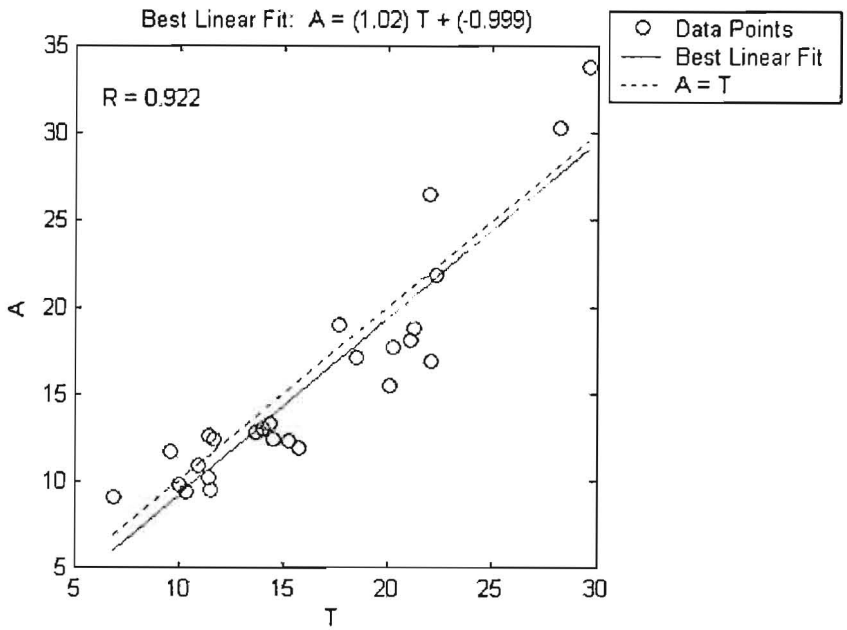

Figure (5-13): The correlation between the large placental vessels (N) predicted using (T) the network with the radius as input and (A) the network with the radius as output.

T = Value for N predicted with the NN using Doppler indices and umbilical radius as input

A = Value for N predicted with the NN using only Doppler indices.

5-5 Summary

The foetal model generates a large number of waveforms at both ends of the umbilical artery. This data is then used as a training set to train the neural network. Because the potential of the network is not only to memorise the data in the training set but also to generalise successfully with data that is not involved within the training set, it was necessary to test the network performance on a previously unseen set of clinical data. From this step we are also able to see the effect of the hidden layers and the neurons on the results.

The prediction values from the trained neural network were 3 outputs ur, ul and N. No exact references were available to interpret these factors at the time of this study. The

need was to create centiles of ur and N based on the foetal model data in an attempt to interpret these values for improved evaluation of the foetal condition.

It was impossible to train the neural network from one location of the cord. At least two locations on the cord were required to train the neural network. Training neural network from one location could be improved by measuring reflection coefficient.

Nowadays with Doppler Ultrasound we are able to see the location of the cord easily and we can also measure the radius of the umbilical artery. As a result, the two ends of the cord (i.e. Doppler indices for both sides of the cord) were considered to supply the network with the data, and the radius could also be used as input to the neural network. Using the radius as input, the output did not show a big change, as demonstrated by the high value of the correlation coefficient (R=0.922) as shown in figure (5-13).

Chapter 6. Discussion

6-1 Training Neural Networks Based on Data from the Foetal Model

The foetal model was able to simulate a number of different scenarios of the umbilical blood flow velocity at both ends of the cord as shown in table (4-2). The results from these simulations were the input set and the desired output set used to train various neural networks.

Eleven back propagation neural networks were investigated as agents for pattern recognition in blood flow velocity waveforms. These networks were trained using the training algorithms summarised in table (5-1).

With the initial parameters in place for the networks, as shown in table (4-3), the algorithms traincgf, traincgp, traingdm, trainoss, trainbfg, traingda, traingdx, trainscg and traincgb, did not produce satisfactory results. Regression analysis carried out after training with these algorithms produced low values of the correlation coefficient ($R < 0.9$) and training did not converge to the goal. These algorithms were therefore excluded from our study.

Although trainrp did not meet the performance goal with initial parameters, it did provide a suitable correlation coefficient ($R > 0.9$). To converge this algorithm to the performance goal the number of neurons in the hidden layers had to be increased, simultaneously increasing the epoch number. The problem arising with this algorithm was that training time here was longer than it was with the trainlm algorithm.

Training with the trainlm algorithm was very successful and was completed, in less than 10 epochs, when compared with trainrp which required 1300 epochs. However, the difficulty with this algorithm is that the network with fewer neurons, eg: 4 neurons in the hidden layer, could be trained and converged successfully. As a result, the network is unable to learn the desired output, in other words the performance of the trained network

become less effective (R changed from 0.98 to 0.85). Increasing the neurons in the hidden layers resulted in problems; either an overfitting problem or a memory reduction had to be achieved (mem_reduc is set to 2, then only half of the Jacobian would be computed at one time.).

In most situations, there is no way to determine the best number of neurons in the hidden layers without training several networks and estimating the generalisation error of each. If we have too few hidden neurons, we will get a high training error and high generalisation error due to underfitting. If we have too many hidden neurons, we may get a low training error but still have a high generalisation error due to overfitting.

6-2 Training Neural Networks Based on Real Clinical Data

During learning, the outputs of a supervised neural network come to approximate the target values, given the inputs in the training set. This ability may be useful in itself, but more often the purpose of using a neural network is to generalise, in other words, to have the outputs of the network approximate target values, given inputs that are not in the training set.

The aim of using the neural network was to quantify the physiological patterns in blood flow velocity waveforms for both the foetal model and real clinical data. With the foetal model we could generate thousands of waveforms. The neural network behaved very well with data based on the foetal model as shown in table 5-1 (R=0.988 with Trainlm), the question is whether the network behaves successfully using real clinical data that the network has never previously seen.

In network terminology, the data set is usually divided into three; the training set, the validation set and the test set. Each set then also divides into the input and desired output set. The input set to the neural network based on the foetal model data was (RI_P , PI_P , RI_F , PI_F , FHR , GA) and the output set was (ur , ul , N). With clinical data, the input set had the same dimensions as the previous one, but with the output set the only parameter

of the three that was available was the umbilical radius (ur). So we could not consider the clinical data as part of the test set or validation set because of the differences in the dimension of the output (see appendix A-2 for details of the training, validation and test set).

To overcome this problem, we proposed first creating many neural networks with a different number of neurons in the hidden layers. These networks were then trained based on the data that was obtained from the foetal model as shown in table (5-2). The training stopped when all the networks met the goal performance which was set to be = 1 e-2. When the networks met the goal, the trained networks were then ready to be tested on the clinical data. According to the performance of these networks on the clinical data, we selected the best networks, which produced the highest performance. The performances of these networks from figures (5-1 to 5-4) are summarised in the following table:

Algorithm	R – correlation coefficient Between true ur and NN predicted ur.
Trainlm with 2 HL	0.705
Trainlm with 1 HL	0.711
Trainrp with 2 HL	0.651
Trainrp with 1 HL	0.746

Table (6-1) : Summary of the Performance of the Networks Based on the clinical data (26 cases) using the correlation coefficient between the true ur and that predicted using the NN.

The effect of the hidden layers was reported and it was demonstrated that in multilayer perceptrons (MLPs), with any of a wide variety of continuous non-linear hidden-layer activation functions, one hidden layer with an arbitrarily large number of neurons suffices for the "universal approximation" property (Hornik et al. 1989). Furthermore, (Heaton

2004) reported that for many practical problems there is no reason to use any more than one hidden layer. Problems that require two hidden layers are rarely encountered.

From table (6-1), we observed that the network with one hidden layer and more neurons within the hidden layer performs more efficiently than two hidden layers either with the trainlm or trainrp algorithms.

No exact theory exists to tell us how many hidden units are needed to approximate any given function. It was therefore necessary to change the number of neurons in the hidden layers by trial and error in an attempt to reduce both the training error and the generalisation error.

6-3 Location of Measurements along the Umbilical Cord

Many researchers have been faced with the dilemma of which position to perform flow measurements at along the cord. Jacques et al (1989) reported that the two ends of the cord yield significant statistical differences in Doppler indices. It was furthermore reported that normal values were obtained from the placental insertion, with higher values being recorded at the foetal abdominal insertion, in the same patients.

(Trudinger et al. 1985) took measurements at two different sites on the cord, but did not establish any significant difference.

(Mine et al. 2001) concluded that a major difference exists between the umbilical arterial flow velocity waveforms on the foetal and placental sides, which might be caused by a difference in umbilical arterial resistance.

6-3-1 Our Explanation

Actually, there is a finite difference between the measurements at placental insertion and those of foetal abdominal insertion. Nonetheless, these differences are sometimes quite

difficult to observe with the naked eye. A tool powerful enough to differentiate between these two locations was therefore needed.

The neural network is used not only for its ability to find a solution, where the physical processes are not understood or are highly complex, but is also employed due to its remarkable capacity to derive meaning from complicated or imprecise data, which is too complex to be noticed by either humans or other computer techniques. (Stergiou and Siganos, 1996).

Training neural networks based on one location of the umbilical artery was impossible see figure (5-8, 5-9). We left the network to train for about 7 or more hours on each side of the cord. The result was that the network did not converge to the performance goal. We performed many trials with a view to improving the training, such as increasing the number of neurons or number of hidden layers or pre-processing the data see appendix (A-3) before training, but the result remained that the training did not converge. The solution then was to provide the network with data from two locations instead of one. This resulted in the network training very successfully in less than 2 minutes figure (5-10). But the question here is, what took place that allowed the neural network to train successfully?

A possible explanation is that there is inadequate information from one location of the cord. In other words, different training data sets will produce the same RI and PI value, at one location. However, due to wave reflection and travel along the cord, these same training sets produced different patterns of RI and PI values along the cord.

Maulik (1993) reported that the existence of wave reflections in the circulatory system is evident from the observation that, as one samples along the arterial tree from the heart to the periphery, the pulsatility of pressure waves progressively increases and the pulsatility of the flow , or flow velocity waves, declines. As a result, pressure and flow waves acquire distinctly different configurations as they propagate down the arterial tree.

These findings led us to study Transmission Line Theory to establish whether there is a relationship between wave reflection and the measurements taken from both ends of the line.

Appendix (B) explains the wave reflection phenomenon and shows the solution of the transmission line equation at both ends of the transmission line; the result shows that the pressure wave at both locations of the line depends on the reflection coefficient, RC, as follows:

$$V(x=0) = V_1\left[1 + RC\, e^{-2\gamma L}\right] \qquad 6\text{-}1$$

$$V(x=L) = V_1\, e^{-\gamma L}\left[1 + RC\right] \qquad 6\text{-}2$$

Here x = 0 represents the foetal abdominal insertion and x = L represents the placental insertion. The same thing can be performed with the current (i.e. blood flow).

Table (5-3) shows that training the neural networks based on one location where the input to the neural network is (RI_P, PI_P FHR, GA) or (RI_F, PI_F, FHR, GA) is not sufficient, as proved in section (5-3-1). The solution to this problem is only possible when using the reflection coefficient as an input, together with indices from either one of the ends of the cord figures (5-11, 5-12). But clinically there is no way of calculating the reflection coefficient. Therefore the only way available to solve this issue clinically is to use more than one measurement site.

6-4 Discussion. The Clinical Data

The performance of the networks for 26 cases was satisfactory as shown in table 6-1. Using the correlation coefficient for each of the networks it was about 0.7.The highest being the network with the trainrp algorithm with one hidden layer which was R=0.746.

Although 26 umbilical waveforms were obtained clinically, the most important of these physiological factors are not known. Factors can be predicted using the trained network

and they are: the umbilical radius (ur), umbilical length (ul) and the number of large vessels (N).

The need thereafter was to find a way to interpret the meanings of these factors. We thus created the centiles of the variables N and the umbilical radius as shown in figures (5-6, 5-7). The discussion of these 26 cases will be clarified later in this chapter.

However, we mentioned in section (4-4) that there were 3 cases, which were excluded from the analysis shown. These cases had reverse or absent flow.

When the trained neural networks were presented with these cases, the networks, based on the foetal model data, predicted that the umbilical radius was higher than that measured clinically with ultrasound as shown in the highlighted box in the following table:

The input to network 2							Scenario 1		Scenario 2
The input to network 1						Clinical radius cm	Network 1 Predicted		Network 2 Predicted
R_p	P_p	R_f	P_f	FHR	GA	ur	ur	N_1	N_2
1	2.6	1	2.65	154	29	.13	.22	10.4	3.4
1	2.24	1	2.06	140	28	.115	.228	11.7	2.5
1	2.52	0.87	1.87	148	30	.16	.38	22.9	9.2

Table (6-2): Summary of simulation of the trained neural network with the 3 cases,
network 1 predicts the radius as output and
network 2 uses the radius as input and it predicts the value of N

Note: the last two simulations with network 1 and network 2, as shown in tables (6-2), were performed based on the network with the trainrp algorithm with one hidden layer.

We chose to use this network because of the high performance it previously produced R=0.746.

We mentioned, in section (5-4) that the umbilical radius could be used as input to the network with other inputs. The results were that the network trained much faster compared with the one that was associated with the radius as output. Moreover, the correlation coefficient between the predicted values N from this network and the other N that was produced from the network, that used the radius as output, was high R=0.922 as shown in figure (5-13). Because the correlation between both N's is high, there is no significant difference in results when using the radius as input or output.

However, this is not the case with the three instances where the predicted values of N_1 and N_2 as shown in table (6-2) are significantly different $P<0.05$.

6-4-1 Explanations of High RI Value

The problem, that is associated with absent or reverse flow and the network is probably due to the ultrasound equipment itself. This machine usually has a filter to cut off low frequencies (to reduce movement artifact), but this filter also corrupts frequencies in the range of absent or reverse flow. As result the RI is saturated at 1, after which point it ceases to yield further information as shown in table (6-2). This situation led network 1 to mislead us in the decision-making.

The two networks in table (6-2) illustrate two different scenarios for obtaining a high value of RI (i.e. RI =1). By plotting the values of N_1, N_2 and the umbilical radius on graphs (5-6, 5-7) for network 1 and 2, we were able to monitor the condition of both the placental resistance and the umbilical radius. However, in the first scenario network 1 predicted that the placental resistance would be normal or just about normal. At the same time network 1 also predicted that the radius would be very high. As a result, the proportion of terminal impedance of the placenta to the characteristic impedance of the umbilical artery became very high. Therefore the resistance index RI increased to RI=1

as shown in table (6-2). The second scenario for obtaining absent flow or reverse flow prevails when the placental resistance is extremely high (i.e. placental vascular pathology). As a result the resistance index increases. This was obvious when using the radius as input to neural network 2. The predicted values of N_2 from network 2, which represent the opposite side of the placental resistance, were very small and the placental resistance was very high. As result of saturation of RI the neural network 1 failed to predict the second scenario. Nevertheless, the network 1 simultaneously predicted the correct conditions for high RI value (i.e. normal placental resistance associated with high umbilical radius produces a high value of RI).

6-4-2 The Contradiction Between Doppler Results and Clinical Outcome

Doppler indices for a number of the 26 pregnant women, who either have pre-eclamplsia or hypertension, were normal. The question that needs to be posed is whether the placenta is in fact functioning normally when normal umbilical arterial waveforms are recorded (i.e. RI in the normal range)?

In a study of pre-eclamplsia (Cameron et al. 1988), it was found that 70% of cases had normal umbilical artery indices with no clear correlation between Doppler indices and levels of hypertension.

An increase in placental resistance is commonly assumed to be the cause of abnormal waveforms in growth-restricted foetuses from pre-eclamptic pregnancies (Trudinger 1987). Furthermore, in a study of severely growth restricted foetuses with near zero end-diastolic velocities, Jackson et al. (1995), failed to detect a placental vascular pathology that markedly increases resistance. Surat and Adamson (1996) suggested that in some cases, factors other than increased placental vascular resistance may be involved. In particular, they found that the umbilical arterial radius had a profound effect on the flow pulsatility, in cases of normal placental resistance.

6-4-3 Our Explanation of this Contradiction

We ran the foetal model to plot the relationship between N and RI at different values of the umbilical radius as shown in figure (6-1).

The vertical dotted line in figure 6-1 was plotted for a very small value of N, which represents a high value of placental resistance. If the umbilical radius is assumed to be 0.15cm (in the normal average range for a foetus at 28 weeks GA) the resistance index is high 0.9.At the same time the reflection coefficient is also high.

If we hypothesise that vasoconstrictor hormones would be present in the foetal circulation, which constrict the umbilical artery, then the umbilical vascular resistance increases. At the same time the characteristic impedance of the umbilical artery increases and the reflection coefficient is reduced. Therefore, with umbilical vasoconstriction, the point on the dotted line will move from the high value of RI to a lower value of RI (from position 1 to position 2). This phenomenon would tend to hide the abnormality of the placental resistance (or placental pathology).

Graph (6-3) also illustrates that if the placenta is functioning normally and the umbilical artery is dilated for some reason, an increase will occur in the ratio of the placental impedance to the characteristic impedance of the cord due to the decrease in the vascular resistance of the umbilical artery. A result is that the value of the RI will increase to its highest value even though the placental resistance is normal.

This explains why we have to use the umbilical radius as an input with other inputs to the neural network with a view to illustrating the actual condition of the placenta.

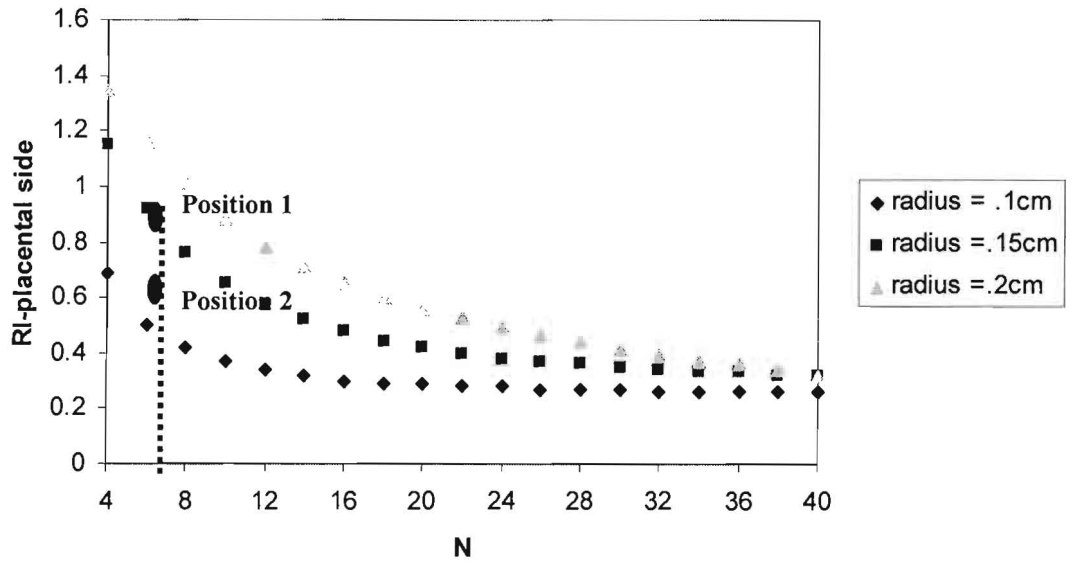

Figure (6-1): The relationship between N and the resistance index RI at different values of the umbilical radius (generated from the foetal model).

6-4-4 Observations from the 26 Cases

Concerning the cases not associated with absent or reverse flow, we mentioned in section (5-4) that there was no difference in the output values of 'N', whether using the umbilical radius as input or not to the network. This was clear from the high correlation coefficient as shown in figure (5-13). To be more accurate the 26 cases will be analysed based on the radius as input to the network.

The trained network, with the umbilical radius as input, will simulate the 26 cases, excluding the three with absent end diastolic flow. The predicted values of N for the 26 cases are shown in the second column of table (E-3) of appendix E.

By plotting the values of N on the centile graph (5-6) we were able to interpret the value of N according to the normality or abnormality of N on this graph.

The Conditions of RI

A normal RI would be produced if the placental resistance was normal (i.e. N normal 'N') and also if the placental resistance was low (i.e.: N is large 'H'). Lastly, if the placental resistance was high (i.e. N is low 'L') a high value of RI would be produced. If the RI conditions diverge from these three conditions it means that the umbilical radius is partly responsible for these changes.

The following table shows the interpreted values of N from centile graph (5-6) compared with the clinical RI and the clinical condition of the patient.

Description of the following table (6-3):

1. The second column of this table represents the condition of N on the centile graph.
2. The third column represents the clinical condition of the RI.
3. The fourth column represents the interpretation of N according to the previous three conditions. Then the interpreted value of N will be compared with the clinical condition of RI to see whether it agrees or not.
4. The last column represents the condition of the pregnant women, which the hospital provided us.

Clinical condition
- N: normal .
- PET : pre-eclampsia
- HT: hypertension, OW overweight baby
- U-inf: infection of the cord

	Interpretation of N	RI_F-at foetal side from the hospital	Correspondence of N and RI_F	Clinical Condition
1	N	N	Agree	N
2	L	H	Agree	PET
3	L	H	Agree	PET
4	H	N	Agree	OW
5	L	H	Agree	U-inf
6	L	H	Agree	HT
7	L	H	Agree	HT
8	L	H	Agree	PET
9	L	N	Disagree	PET
10	L	N	Disagree	PET
11	N	N	Agree	PET
12	N	N	Agree	PET
13	L	N	Disagree	PET
14	N	N	Agree	PET
15	L	H	Agree	PET
16	L	H	Agree	PET
17	H	N	Agree	HT
18	N	N	Agree	N
19	N	N	Agree	N
20	N	N	Agree	N
21	L	N	Disagree	N
22	N	N	Agree	N
23	L	H	Agree	N
24	N	N	Agree	N
25	L	H	Agree	N
26	L	N	Disagree	N

Table (6-3): Illustrates the compression between the situation of N on the centile graph (5-6) and clinical RI at the foetal side.

We observed from table (6-3) that the interpretation of N agrees with the clinical condition of the RI according to its three conditions. There are also about 5 cases (highlighted in table 6-3) that disagree with the clinical observation of the RI. These 5 cases are associated with a high value of placental resistance (i.e. N is low), which according to the conditions of the RI, means that they are supposed to produce a high value of RI. But that did not happen and the result of the RI was normal. The reason for this might be due to the constriction of the umbilical radius as discussed earlier in figure (6-1).

When we plotted the values of the umbilical radius of these 5 cases on centile graph (5-7), we found that all of the 5 radii were below average and some of them had a very small radius especially (9 and 13). Once again this scenario, which is associated with a high placental resistance and a low umbilical radius, masks the actual condition of the foetus and the placenta.

6-4-5 The Difficulties Faced With Clinical Data

1) Doppler ultrasound allows us to measure the umbilical radius. Nevertheless, this factor could contain an error, either because of the resolution of the machine itself or from the pulsatility of the umbilical artery that is associated with the cardiac output.
2) We only had one opportunity to measure the pregnant women. Facilities to repeatedly take measurements or see the same patients again were not available. For this reason, there may have been undetected measurement errors.
3) The present Doppler equipment is only able to perform a measurement at one location on the cord at a time. As a result, there is a period of time which lapses between the measurements taken at the two locations. It is possible that physiological changes occur during this time, such as changes in blood flow distribution, foetal movement or cardiac output. We did not have the facilities to use two Doppler machines simultaneously, which would have enabled us to measure both locations immediately, thereby avoiding delays. If the cardiac

output changes, we reperformed the measurements. Otherwise, we had to assume that the foetal circulation was unchanged, between the two measurements. Any changes, would thus result in this assumption being violated, and would cause errors.

4) We found the Doppler indices of some patients to be higher at the placental side than at the foetal side. A possible explanation could be as a result of a very high umbilical radius and normal or low placental resistance. This scenario has been shown (using the foetal model) to result in higher DI values at the placental side than at the foetal side of the cord. It has also been observed from the clinical data of some cases that RI at the placental side is greater than RI at the foetal side. These cases (1, 4 and 17) are illustrated in table 6-3. This was as a result of a very high value of the umbilical radius and low placental resistance (i.e. a very large value of N). Another explanation could be as a result of point 3 above, where physiological changes over time may have resulted in differences, rather than these being caused by the different sites of measurement.

5) The few results of clinical outcomes we obtained, were supplied to us by the hospital. Interestingly, two cases in particular, were associated with a high value of RI; one was associated with absent flow as shown in table (6-2) case number 2 and the other was shown in the table (6-3) case number 6 were both associated with a very low value of the umbilical radius and a high value of the placental resistance (i.e. N small). Both of these cases suffered from foetal distress and ended up with caesarean sections. We noticed that in cases of a high RI and a low value of the umbilical radius, the foetuses were at increased risk of foetal distress. Therefore, monitoring the umbilical radius when the RI is very high might be one of the early warnings to avoid the effects of foetal distress. Further investigation into the effect of the umbilical radius in case of high values of RI is required in future research.

6) In the foetal model we had to assume that the umbilical cord grew normally. The reason for this was because we were not able to obtain the cord length of the 29 women, from the hospital after delivery. Additional investigation will be required

into the use of umbilical cord length as a variable factor, like others such as the umbilical radius and FHR.

7) The centile graph that was obtained from Tygerberg hospital, as shown in figure (5-5), was used in the hospital to investigate the condition of the RI at the foetal side, although its construction had been based on continuous Doppler ultrasound (i.e. With this equipment it is not possible to determine the exact location of the site of measurement on the umbilical cord). We also used this graph to investigate our RI at the foetal side, as the hospital does. But that obviously might not have been correct, as a result of that, table (6-3) and figure (5-6, 5-7) might include some errors. Additional investigation is therefore required for creating two centile graphs of Doppler indices, one for the foetal side and the other for placental side.

6-5 Summary

In this chapter we observed many phenomena that may lead to an explanation of the contradiction surrounding Doppler results and clinical outcomes.

Training the neural network from one site of the cord was impossible. We assumed that as the waves travelled along the cord they would face a reflection wherever there were obstacles. As a result the network was able to train from one location when using the reflection coefficient as input with other inputs to the NN. It is, nevertheless, clinically difficult to measure this factor. Therefore, it was necessary to find another solution, which was done by using more than one location.

We also observed that the umbilical radius plays a very crucial role in identifying the actual condition of the foetus. With absent or reverse flow, we found that the radius is much smaller than average. We also found theoretically, that although the placental functioning was normal, the value of the RI was high. The reason for this is due to the large value of the umbilical radius. The last observation took place when the umbilical radius was small and the placental resistance was high enough to produce a normal value

of RI. So, we suggest using the umbilical radius as an input to the neural network to distinguish between the different scenarios of the RI.

Chapter 7. Conclusion and Recommendation

The measurements of Doppler umbilical arterial blood flow velocity waveforms are widely used in perinatal surveillance. Their usefulness in the management of high-risk pregnancies has been a controversial topic. This controversy served as our motivation to develop an automated system for the interpretation of Doppler umbilical artery waveforms using neural networks in a novel way.

We implemented two applications together, which were adapted to this study. We firstly used the foetal model to generate large numbers of blood flow velocity waveforms at both ends of the cord, secondly we employed backpropagation neural networks that are used to recognise the main physiological patterns associated with these waveforms. The combination of the foetal model and the neural network allowed us to perceive phenomena that would be quite difficult to notice either by the human brain or a normal computer programme.

Eleven algorithms of backpropagation neural networks have been developed as agents of pattern recognition of the blood flow velocity waveforms. Of the eleven algorithms, the neural network only trained successfully with trainlm and trainrp.

Training neural networks with the trainlm algorithm has proven, in this study, to be one of the fastest algorithms of the 11. This algorithm, however, depends mainly on the capacity of the computer. If the computer's memory is problematic it is necessary to use another algorithm like the trainrp algorithm.

It is preferable to use complex networks (i.e. many layers and a larger number of neurons) for particular applications so as to reduce the training error that is associated with the training set as was reported by (Bishop 1999). But that is not the case when unseen data is presented to the network e.g. clinical data, the result here is associated with a high generalisation error as a result of overfitting. In this study we found that the network with one hidden layer is more efficient than the network with two hidden layers.

But the number of neurons in the hidden layer is problematic because there is no exact theory yet to tell us how many neurons are required for each application. However, training many networks with different neurons in the hidden layer and then testing the trained networks on a new data set, represents one of the methods used to measure the network capability in order to reduce the training and generalisation error.

Currently all decision making for the evaluation of the foetal condition is principally based on measurements of the umbilical arterial blood flow velocity waveforms from one site of the cord.

The blood flow, or pressure waveforms as they are travelling from the foetus to the placenta along the cord, will face a reflection wherever they encounter a medium that is different from the medium that they travel through (i.e. difference in the impedance). In our study the primary obstacle is assumed to be the placenta. As a result, there will be both forward travelling and reverse travelling waves in the cord, and these will summate to the final waveform. We found that if we fed the network from one location only, it could not be trained. We propose training the network successfully according to wave reflection phenomena to use either more than one location of the cord or to use the reflection coefficient if it could be measured. It is clinically difficult to measure the reflection coefficient. We concluded that it is much easier to train the network using more than one location on the cord. Because both ends of the cord are much easier to see with Doppler ultrasound, it is preferable to use the placental insertion site and the foetal abdominal insertion site.

The umbilical radius associated with absent or reverse flow was measured clinically by Doppler and found to be very small. But the neural network predicted the umbilical radius to be large with almost normal placental resistance. To avoid this discrepancy, Doppler ultrasound enables us to measure the radius of the umbilical artery. We proposed using the umbilical radius as an input, together with other inputs to the network. The result was that the network predicted that the placental resistance for these women with absent or reverse flow was very high. We could not confirm which of the network's

decisions were correct because we were unable to obtain information regarding the condition of the post partum placenta from the hospital.

If placental resistance is high, the resistance index RI is predominantly high. But that is not the situation in all cases. The combination of the placental resistance and the umbilical vascular resistance has an effect on the value of RI. If the placental resistance is high, we assumed that there would be a strong wave reflection and as a result of that, the reflection coefficient would be high. We also assumed, in this situation, that there would be an agent in the foetal circulation working to constrict the umbilical radius (e.g. the existence of vasoconstrictor hormones in the foetal circulation). As a result of this, RI decreases and might reach normal values. This situation was observed in a number of women in our study. We conclude that the use of Doppler indices from both ends of the cord together with the umbilical radius is necessary to assess the true condition of the placental circulation.

Recommendation

The recommendation has been summarised in the following steps:

1. Decision making for the foetal condition should be based on measurements of the umbilical flow velocity waveforms at both ends of the cord.
2. To measure the blood flow velocity waveform at both ends of the cord simultaneously we recommend using two pieces of ultrasound equipment; so as to avoid any delay between the two measurements.
3. We recommend creating centile graphs for Doppler indices at both ends of the cord with gestational age in order to identify the actual condition of the foetus.
4. We only obtained a few cases of absent and reverse flow. For reconfirmation of our findings we recommend studying more clinical waveforms associated with absent and reverse flow while at the same time studying the effect of the umbilical arterial radius on the umbilical waveforms.

5. We mentioned earlier that the umbilical length was assumed to be normal in the foetal model at each gestational age. But that might not be the actual situation in all cases. A better way is by changing the length in the foetal model and comparing the predicted length with the real clinical length. So we recommend extra analysis based on changing the umbilical length.
6. In the foetal model, the effects of vessel tapering and coiling in the vessels have not yet been considered. Therefore, extra analysis is required involving these cases in the model for better understanding of the foetal circulation.

Appendix A Matlab

A-1 Introduction

The term Matlab, which stands for 'matrix laboratory' is an interactive system. Originally it was written as software for matrix computation but has changed and grown with time to serve as a didactic aid in mathematics, engineering and science courses. It is also employed for research, development and analysis. Matlab toolboxes consist of an assortment of functions used to solve particular classes of problems. Signal processing, control system, fuzzy logic, wavelets, simulation and neural networks are areas where toolboxes are available. (MathWorks , Inc .2004).

A-2 What is the Training Set, Validation Set and Test Set?

The available data is divided into three groups: training set, validation set, and test set. The training data is used to adjust the weights between neurons in the neural network. The validation set is used to monitor the convergence of the training, and to ensure that the neural network can generalize for data, on which it was not trained. The test set is used to test the neural network's ability to predict pavement performance on new data.

A-3 Training Set

A single matrix of concurrent vectors is presented to the network and the network produces a single matrix of concurrent vectors as output. This is the batch mode form, in which all of the input vectors are placed in one matrix. This is much more efficient than presenting the vectors one at a time (incremental mode).

The matrix that is presented to the networks table (5-1) consists of rows and columns. Each row represents a different element. These elements are (RI_P, PI_P , RI_F , PI_F , FHR , GA), which represent the number of neurons in the input layer, and the columns or the vectors of this matrix represent different values of these elements. The number of vectors in this matrix is equal to the number of waveforms that were generated from the foetal

model (2268). The number of elements for the matrix that is produced from the networks is three ur, ul and N, this number represents the number of neurons in the output layer. The number of vectors for the output matrix is 2268.

The networks in table (5-1) were first trained without any pre-processing of the training set and the result was that the networks did not train based on one location. Then, in order to make the neural networks train more efficiently, they were pre-processed. One of the pre-processing techniques available is a procedure that scales the network inputs and targets by normalising the mean and standard deviation of the training set. The inputs and the targets are normalized so that they have zero mean and unity standard deviation. The other technique of pre-processing the training set is to scale the data so the minimum is -1 and the maximum is +1.

Although the training set was pre-processed in different ways, the network did not show any progression for training from one location.
The Matlab functions that are used for pre-processing methods are:
prestd: Pre-processes the data so that the mean is 0 and the standard deviation is 1.
premnmx: Pre-processes data so that minimum is -1 and maximum is 1.

A-4 Creation Feed Forward Neural Network

The following function describes creating the feed forward network:
net = newff (mm, sizeArry, transferFunctionCellrray, trainingAlgorithm); A-1
net : the neural network to be created (the name 'net' is changeable)
mm: Matrix of size number_of_inputs × 2. Each row contains the minimum and maximum value that a particular input (or element) can have.
sizeArray: Array that contains size for each layer (not including input)
transferFunctionCellArray: Cell Array that contains strings representing the transfer functions for each layer (not including the input layer).
The following table shows the different transfer functions that are provided by Matllab

Transfer function	Matlab String
Logarithmic sigmoid	logsig
Tangential sigmoid	tansig
Linear (identity function)	purelin

Table A-1: the transfer functions provided by Matlab

Transfer or activation functions for the neurons in the hidden layer are needed to introduce non-linearity into the networks. The reason for this is that a composition of linear functions is a linear function. However, it is this non-linearity (i.e. the capability to represent non-linear functions) that renders multi-layer networks so powerful. Almost any non-linear function does the job, although for back-propagation learning it must be differentiable .The sigmoid functions (logsig or tansig functions) are the most common choices.

For the output units, transfer functions should be chosen to be suited to the distribution of the target values. For binary [0,1] outputs, the sigmoid function is an excellent choice. For continuous-valued targets with a bounded range, the sigmoid functions are again useful, provided that either the outputs or the targets be scaled to the range of the output activation function. But if the target values have no known bounded range, it is better to use an unbounded activation function, most often the identity function (purelin function).

Training Algorithm: A string representing the training algorithm for the network. The following table shows the variety of Training algorithms of backpropagation that are provided with Matlab NN toolbox.

Training algorithm	Matlab String
Conjugate gradient backpropagation with Fletcher-Reeves updates.	Traincgf
Conjugate gradient backpropagation with Polak-Ribiere updates.	Traincgp
Resilient backpropagation	Trainrp
Gradient descent with momentum backpropagation.	Traingdm
One step secant backpropagation.	Trainoss
BFGS quasi-Newton backpropagation.	Trainbfg
Gradient descent with adaptive lr backpropagation.	Traingda
Gradient descent w/momentum & adaptive lr backpropagation.	Traingdx
Scaled conjugate gradient backpropagation.	Trainscg
Conjugate gradient backpropagation with Powell-Beale restarts.	Traincgb
Levenberg-Marquardt backpropagation.	Trainlm

Table A-2: Bakpropagation training algorithms provided by Matlab

The previous list summarizes the training algorithms included in the Matlab toolbox. This table illustrates different backpropagation training algorithms. They have a variety of different computation and storage requirements, and no one algorithm is best suited to all locations.

When the network is created, it is then ready for training:

Training function:

[net] = tarin(net, P, T, [], [], VV, TT); A-2

net : neural network to be trained.

P : Network inputs

T : Network targets (desired outputs)

VV: Structure of the validation vectors

TT: Structure of the test vectors

[]: Because the network is static the network delay is zero as shown in the training function as an empty matrix [].

Because we did include validation or test set the training function can be simplified as:

[net] = tarin(net, P, T); A-3

Once the network trained, thereafter the network can be tested by a simulation function as following:

Output = sim (net, testdata); A-4

net: network to be tested

testdat: testing data set.

Section (3-6) illustrated a method by which the trained neural network performance can be measured using the regression analysis. In Matlab there is a function allows us to calculate the regression coefficient immediately as following:

[m,b,r] = postreg(A,T) ; A-5

postreg: Postprocesses the trained network response with a linear regression.

postreg(A,T) takes these inputs,

A - 1xQ array of network outputs. One element of the network output.

T - 1xQ array of targets. One element of the target vector.

and returns,

m - Slope of the linear regression.

b - Y intercept of the linear regression.

r - Regression R-value. R=1 means perfect correlation.

Appendix B Transmission Line Theory

The Foeto-placental circulation could be represented by a transmission line system, where the umbilical artery represents the line and the placenta represents the terminal impedance of the line as shown in figure (B-1).

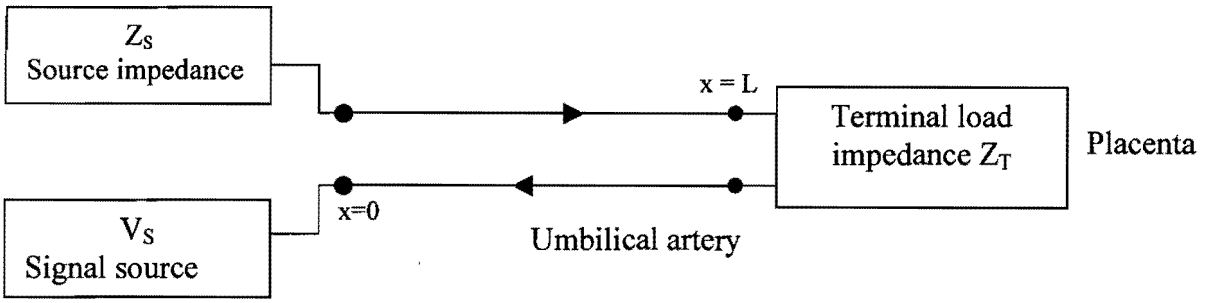

Figure (B-1): Basic Transmission Line Circuit, where waves are reflected from the impedance Z_T. The line length is L.

Wave reflection: this phenomenon is very similar to the cases of light waves, sound waves and water waves: Whenever travelling waves meet an obstacle (i.e. encounter a discontinuity in the medium in which they have been travelling), they are partially or totally reflected. Furthermore, the reflected wave then travels in the opposite direction and interacts with the incident wave to create a different pattern along the line.

When a uniform transmission line is terminated in an impedance equal to its characteristic impedance, there are no reflected waves on the line, and the impedance at any point of the line, including the input terminals, is also equal to the line's characteristic impedance.

When a uniform transmission line is not terminated in its characteristic impedance, but is terminated with some arbitrary impedance $Z_T \neq Z_0$, there are always reflected waves on the line, and the impedance at every point of the line differs from the characteristic impedance Z_0.

When an incident arterial pressure wave V_1 encounters a load impedance Z_T not equal to the characteristic impedance Z_0 of the umbilical artery, wave reflection occurs. A reflected wave V_2 then travels in the opposite direction and interacts with the incident wave V1 to create a different pressure waveform V.

In the foetal model, the pressure is represented by the voltage and the blood flow through the circulation is represented by the current in an electrical transmission line.

Referring to the general equation of the Transmission line theory (Chipman 1968)

$$V(x) = V_1 e^{-\gamma x} + V_2 e^{+\gamma x} \qquad \text{B-1}$$

$$\gamma = \alpha + j\beta \qquad \text{B-2}$$

Where V_1 refers to a forward travelling wave and V_2 to a reverse travelling wave. Whose values are obtained by the pressure and internal impedance of the signal source connected at x = 0, the attenuation and phase factors of the line α and β respectively, the line length L, and the terminal load impedance Z_T connected at x=L.

In any discussion of reflected wave phenomenon, whether the wave is sound waves, water waves, light waves, etc., the concept of a 'reflection coefficient' is introduced.
The natural definition of such a concept is:

Reflection Coefficient (RC) = Value of reflected wave at point of reflection (x = L) /
Value of incident wave at point of reflection (x = L)

$$RC = \frac{V_2 e^{\gamma L}}{V_1 e^{-\gamma L}} \qquad \text{B-3}$$

$$V_2 = RC\, e^{-2\gamma L} V_1 \qquad \text{B-4}$$

From equation B-4 and B-1 we obtain on the following

$$V(x) = V_1 e^{-\gamma x} + V_1 RC e^{\gamma(x-2L)} \qquad \text{B-5}$$

$$V(x) = V_1\left(e^{-\gamma x} + RC e^{\gamma(x-2L)}\right) \qquad \text{B-6}$$

The pressure wave at the foetal abdominal insertion of the cord (x=0) is calculated as

$$V(x=0) = V_1\left(1 + RC e^{-2\gamma L}\right) \qquad \text{B-7}$$

The pressure wave at the placental insertion of the cord (x=L) is calculated as

$$V(x=L) = V_1\left(e^{-\gamma L} + RC e^{-\gamma L}\right) \qquad \text{B-8}$$

$$V(L) = V_1 e^{-\gamma L}(1 + RC) \qquad \text{B-9}$$

The same thing will be performed with the current or the blood flow.

Appendix C Matlab Programs

All of the following programs for the neural network have been written in Matlab language.

Disk A, attached to this thesis, contains the programs that have been performed on the neural network.

The following networks represent the different networks that have been successfully trained with trainlm and trainrp algorithms based on the foetal model data and tested on the clinical data as shown in figures (5-1, to 5-4).

The input to these networks will be (RI_P, PI_P, RI_F, PI_F, FHR , GA) and the outputs will be (ur,ul, N).

net1: represents the neural network trained by trainlm with two hidden layers.
net2: represents the neural network trained by trainlm with one hidden layer.
net3: represents the neural network trained by trainrp with two hidden layers.
net4: represents the neural network trained by trainrp with one hidden layer.
The following network represents the trained network based on the radius as input. The input to this network will be (RI_P, PI_P, RI_F, PI_F, FHR , GA + the umbilical radius 'ur') and the output will be ul and N only.
net5: represents the trained network based on the radius as input to the network.

If we have a new data set the only thing it will do is to simulate the new data to these networks (net 1 to 5) by using the simulation function (A-4) and then obtaining the output.

Prog1: This program was set up to train the network based on two locations of the cord and based on the data from the foetal model table (4-2). Also, by changing the parameters of the input set (i.e. a matrix x1 as shown in this program), we can change the program to

become accustomed to training the network based on one location or training the network based on one location of the cord with a reflection coefficient 'RC'.

This program includes the data that was generated from the foetal model (i.e. the input and the desired output vectors 2268 waveforms). Furthermore, this program shows all the calculations of the functions that were mentioned earlier in appendix A about creating, training, pre-processing, etc of the network.

Prog2: The networks that are generated from Prog1 are tested here on a new data set (i.e. clinical data). The performance of the trained network is measured using the regression analysis. This program also shows the clinical data set of 29 pregnant women.

Prog3 : This program is divide into two parts:
The first part is used to filter the data that was generated from the foetal model (i.e. changing the values of N or umbilical radius with keeping the other factors constant). The result from this step is the normal values of N at different gestational ages.
The second part is used to calculate the centiles of N.

The results of this program will be transferred to Microsoft Excel to plot the centile graph (N or ur vs. GA) as shown in figures (5-6, 5-7).

Appendix D The Main physiological Patterns

Simulation parameter (for a 50% decrease)	Sensitivity of index		Difference between ends	
	Normal placenta	CPI	Normal Placenta	CPI
Acute placental insufficiency (API)	H↑	N/A	H ↑	N/A
Chronic placental insufficiency (CPI)	H↑	N/A	M↑	N/A
Heart rate	H↑	H↑	↔	↔
Cardiac output (acute)	L↑	M↑	↔	H↓
Cardiac output (chronic)	L↑	L↑	↔	↔
Blood pressure (acute)	L↓	L↓	↔	↔
Blood pressure (chronic)	L↓	L↓	↔	↔
Umbilical arterial elasticity	L↑	L↑	M↑	M↑
Umbilical arterial wall thickness	L↓	L↓	M↑	M↑
Wharton jelly	L↓	L↓	H↓	H↓
Umbilical arterial wall visco-elasticity	L↓	L↓	H↓	H↓
Placental vessel elasticity	L↑	L↑	↔	H↑
Placental vessel wall thickness	L↓	L↓	↔	↔
Placental vessel wall visco-elasticity	L↑	L↑	↔	↔
Total foetal blood viscosity (acute)	M↑	M↑	↔	↔
Total foetal blood viscosity (chronic)	M↑	M↑	↔	↔
Acute redistribution	L↑	L↑	↔	↔
Umbilical radius (acute)	H↓	H↓	H↓	H↓
Umbilical radius (chronic)	H↓	H↓	H↓	H↓
Umbilical radius (sheep experiment)	M↓	N/A	H↓	N/A
Umbilical length	H↑	H↑	H↓	H↓
Coiling 28 weeks	L↓	N/A	↔	N/A
Coiling 40 weeks	L↓	N/A	↔	N/A
Coiling low alpha	L↓	N/A	↔	N/A

Table D-1: the main physiological patterns (Myers 2001, Capper and Myers 2003).

Table (D-1) is a summary of simulated changes in each variable listed under simulations. For index sensitivity, L denotes a low change (<10 %), M a medium change (>10%, <30%) and H a high change (>30%). For the differences between the ends of the cord, a different scale is used and here M denotes a medium change (>10%, <100%) and H a high change (>100%). Anything less than 10% is insignificant and assumed to be equal. A ↓ symolises a decrease in index or difference in indices at either end of the cord, a ↑ symbolises an increase and ↔ symbolises no change in differences. Simulations are for a normal placenta and for a situation of chronic placental insufficiency (CPI). Plcaental changes are for decreased flow to the placenta .

Appendix E Simulation of the Network

The data that is shown in the following tables was generated from the simulation of the clinical data on the trained neural networks. This simulation was performed on the networks that are mentioned in Appendix C (net1, 2, ...and 5).

'N' predicted by the Neural Network			
Trainlm with 2 HL	Trainlm with 1 HL	Trainrp with 2 HL	Trainrp with 1 HL
12.0	11.8	17.8	14.4
12.7	15.3	12.8	11.4
11.0	16.3	17.2	10.0
30.4	27.9	30.0	29.6
14.0	15.5	13.4	14.0
13.9	13.7	12.6	11.4
19.7	21.3	17.4	17.6
9.9	10.8	11.5	12.1
14.6	16.1	14.1	13.7
22.5	23.7	20.4	21.2
22.8	23.1	21.5	22.0
15.6	18.6	22.0	15.8
16.2	19.1	16.6	15.3
21.5	22.9	21.8	21.1
9.4	10.3	6.5	6.9
10.4	11.6	9.7	11.0
26.0	25.5	26.3	28.2
13.4	15.6	16.3	11.7
22.7	24.0	24.4	22.1
21.8	21.9	21.8	22.3
19.7	20.2	19.2	18.5
9.8	10.5	10.6	9.6
17.1	17.9	15.9	14.5
19.8	20.5	24.8	20.2
10.0	10.4	9.7	10.4
19.4	19.6	20.5	20.1

Table (E-1): N (large vessels) values generated from simulation of networks with 1 HL and 2HL and with both trainrp and trainlm algorithms (based on clinical data).

	Radius predicted by the Neural Network.			
Real clinical radius	Trainlm with 2 HL	Trainlm with 1 HL	Trainrp with 2 HL	Trainrp with 1 HL
0.36	0.39	0.42	0.50	0.39
0.35	0.39	0.41	0.37	0.38
0.35	0.40	0.44	0.45	0.36
0.48	0.48	0.57	0.56	0.54
0.39	0.39	0.40	0.37	0.40
0.29	0.31	0.31	0.30	0.30
0.42	0.42	0.44	0.40	0.43
0.34	0.34	0.38	0.39	0.38
0.35	0.37	0.37	0.37	0.37
0.38	0.45	0.47	0.41	0.45
0.43	0.41	0.43	0.38	0.41
0.33	0.40	0.45	0.51	0.43
0.31	0.33	0.37	0.33	0.33
0.38	0.43	0.46	0.42	0.43
0.35	0.29	0.26	0.25	0.27
0.41	0.39	0.41	0.38	0.39
0.46	0.46	0.51	0.45	0.48
0.34	0.36	0.37	0.37	0.34
0.39	0.47	0.52	0.50	0.50
0.38	0.39	0.42	0.38	0.39
0.39	0.45	0.46	0.43	0.44
0.34	0.27	0.27	0.27	0.29
0.37	0.47	0.47	0.44	0.46
0.34	0.37	0.40	0.40	0.36
0.30	0.31	0.31	0.31	0.31
0.38	0.48	0.50	0.49	0.49

Table (E-2): ur (umbilical diameter in cm) values generated from simulation of networks with 1 HL and 2HL and with both trainrp and trainlm algorithms (based on clinical data).

1 Trainrp radius as output	2 Trainrp radius as input
14.4	13.2
11.4	10.2
10.0	9.7
29.6	33.8
14.0	12.9
11.4	12.6
17.6	18.9
12.1	9.4
13.7	12.8
21.2	18.8
22.0	26.6
15.8	11.9
15.3	12.3
21.1	18.1
6.9	9.1
11.0	10.9
28.2	30.3
11.7	12.4
22.1	16.9
22.3	21.8
18.5	17.1
9.6	11.7
14.5	12.4
20.2	17.6
10.4	9.4
20.1	15.4

Table (E-3): N (large vessels) values predicted using:

(1.) a NN using only the Doppler indices in the training set and (2) a NN that was used both the Doppler indices and the umbilical radius in the training set.

References

Arduini D. and Rizzo G. (1990). Normal values of pulsatility index from fetal vessels: a cross-sectional study on 1556 healthy fetuses. J. Perinat. Med.,18(3): 165-172.

Ayala K., Ariel J., David E. (1999). Hemodynamic model for analysis of Doppler ultrasound indexes of umbilical blood flow. Am. J. Physiol. (Heart Circ. Physiol.), 276 (6) : 2204-2214.

Beattie R.B. and Dornan J.C., (1989). Antenatal screening for intrauterine growth retardation with umbilical artery Doppler ultrasonography. Br. J. Med., 298(6674): 631-635.

Beksac M.S., Basaran F., Eskiizmirliler S.,Erkmen A.M., Yorukan S., (1995). A computerized diagnostic system for the interpretation of umbilical artery blood flow velocity waveforms. Eu. J. Obstet. & Gynecol. and Reproductive Biology, 64(1): 37-42.

Bishop C.M., (1995). Neural networks for pattern recoginition. Oxford University Press.
Boyd J.D., Hamilton W.J., (1970). The Human Placenta. Cambridge: Heffer & Sons, 207–274.

Bishop C.M., (1999). Pattern recognition and feed-forward networks. The last accessed 2004/12/1.
http://research.microsoft.com/~cmbishop/downloads/Bishop-Networks-MITECS-99.pdf

Cameron A.D., Nicholson S.F., Nimrod C.A., Harder J.R., Davies D.M., (1988). Doppler waveforms in the foetal aorta and umbilical artery in patients with hypertension in pregnancy. Am. J. Obstet. & Gynecol., 158(2): 339-345.

Capper W.L and Myers L An investigation of the determinants of the umbilical Resistance Index using a transfer function model of the foetal-placental arterial system.

The 2003 World congress on Medical Physics and Biomedical Engineering, Sydney convention and Exhibition center, Sydney, August 24-29, 2003.

Davey D.A., MacGillivray I., (1987). The classification and definition of hypertensive disorders, in hypertension in pregnancy (ed sharpe F., Symonds E.M.). Perinatology Press, Ithaca, New York, 401:407.

Dayhoff E. (1990). Neural network arcitectures: Back-error-propagation. Van Nostrand Reinhold, New York. 58:79.

Demuth H., Beale M., (1998). Neural network toolbox user's guide ver. 3 for use with Matlab. Messachusetts: the Mathworks Inc.

Devoe L.D., Gardner P., Dear C., Castillo R.A., (1990). The diagnostic values of concurrent nonstress testing, amniotic fluid measurements, and Doppler velocimetry in screening a general high-risk population. Am. J. Obstet. & Gynecol.,163(3):1040-1048.

Dixon H.G. and Robertson W.B., (1958). A study of the vessels of the placental bed in normotensive and hypertensive women. Br. Emp. J. Obstet. & Gynecol., 65 (5) : 803-809.

Dougherty M., (1995). A review of neural networks applied to transport. Transpn. Res.– C, 3(4), 247-260

Ducey J., Schulman H., Farmakides G., Rochelson B., Bracero L., Fleischer A., Guzman E., Winter D., Penny B. (1987). A classification of hypertension in pregnancy based on Doppler velocimetry. Am. J. Obstet. & Gynecol., 157(3) :680-685.

Ehrenkranz RA, (1976). Effect of ritodrine infusion on uterine and umbilical blood flow in pregnant sheep. Am. J. Obstet. & Gynecol.; 126(3): 343-349.

Erskine R.L. and Ritchie J.W., (1985a). Umilical artery blood flow characteristics in normal and growth-retarded foetuses . Br. J. Obstet. & Gynecol.,92 (6): 605-610.

Erskine R.L. and Ritchie J.W., (1985b). Quantitative measurement of foetal blood flow using Doppler ultrasound. Br. J. Obstet. & Gynecol., 92(6) : 600-604.

Evan Martin and Eileen McLaughlin (2001). Placental insufficiency. The last accessed 2004/11/25.
http://atoz.iqhealth.com/HealthAnswers/encyclopedia/HTMLfiles/2080.html

Fausett L. (1994). Fundamentals of neural network. Prentice hall, New Jersey.

Fleischer A., Schulman H., Farmakides G., Bracero L., Blattner P.,Rudolph G., (1985). Umbilical artery velocity waveforms and intrauterine growth retardation. Am. J. Obstet. & Gynecol., 151(4) : 502-505.

Gagnon R. (2003). Placental insufficiency and its consequences. Eu. J. Obstet. & Gynecol. and Reproductive Biology, 110 (1) : 99-107.

Gagnon R.., Johnston L., Murotsuki J., (1996). Fetal placental embolization in the late-gestation ovine fetus: alterations in umbilical blood flow and fetal heart rate patterns. Am. J. Obstet. & Gynecol., 175(1) : 63-72.

Giles W.B., Trudinger B.J. & Baird P.J., (1985a). Fetal umbilical artery flow velocity waveforms and placental resistance: pathological correlation. Br. J. Obstet. & Gynaecol., 92(1): 31–38.

Giles WB, Trudinger BJ & Cook CM (1985b) Fetal umbilical artery flow velocity-time waveforms in twin pregnancies. Br. J. Obstet. & Gynecol., 92(5): 490–497.

Gill R.W., (1985). Measurements of blood flow by ultrasound: Accuracy and sources of error. Ultrasound in Med. & Biol., 11(4): 625-641.

Griffin D., Bilardo K., Masini L., Diaz-Recasens J.., Pearce J.M., Willson K., Campbell S. (1984). Doppler blood flow waveforms in the descending thoracic aorta of the human fetus. Br. J. Obstet. & Gynecol.; 91(10): 997-1006.

Heaton J., (2004). The number of Hidden layers: Understanding bacpropagation. Last accessed 2004/30/11.
URL http://www.jeffheaton.com/ai/javaneural/ch5.shtml

Helen H., Barbara A., James D., Allen P., Barbara S., (1989). Non-uniformity of foetal umbilical systolic/diastolic ratios as determined with duplex Doppler sonography. Am. J. Ultrasound in Med. & Biol, 8 : 417-420.

Hendrik J, Anderas F, Martin G., Holger K., Alfred K., Heinrich F. (1996). Development of quantitative Doppler indices for uteroplacental and fetal blood flow during the third trimester. Ultrasound in Med. & Biol., 22 (7) : 823-835.

Hertz J., Krogh A., Palmer R.G., (1991). Introduction to the theory of neural computation. Addison-Wesley, New York.

Hornik K., Stinchcombe M., White H., (1989). Multilayer feedforward networks are universal approximators. Neural Networks, 2(5): 359-366.

Kerbs C., Macara L.M.., Leiser R., Bowman A.W., Greer I.A., Kingdom J.C. (1996). Intrauterine growth restriction with absent end diastolic flow velocity in the umbilical artery is associated with maldevelopment of the placental terminal villous tree. Am. J. Obstet. & Gynecol., 175(6) : 1534-1542

Klerfors D.(1998). Artificial neural networks. School of business and administration, Saint Louis University. Last accessed 2004/7/5
URL http://www.secondmoment.org/neuralnets.php

Lack man F., Capewell V., Gagnon R., Richardson B., (2001). Foetal umbilical cord oxygen values and birth to placental weight ratio in relation to size at birth. Am. J. Obstet. & Gynecol., 185(3): 674-682.

Larry Y., Peter A., Knox P., Lesley M. (1988). A transmission line modelling approach to the interpretation of uterine Doppler waveforms. Ultrasound in Med. & Biol., 14(5) : 365-376.

Masters T., (1993). Practical neural network recipes in C++. Academic Press, Inc.

Marsal K., Lindblad A., Lingman G., (1984). Blood flow in the foetal descending aorta. Intrinsic factors affecting fetal blood flow, in fetal breathing movements and cardiac arrhythmia. Ultrasound in Med. & Biol., 10(3): 339:348.

Maulik D. , Yarlagadda AP, Youngblood JP, Willoughby L. (1989a). Components of variability of umbilical arterial Doppler velocimetry--a propective analysis. Am. J. Obstet. & Gynecol., 160(6): 1406-1412.

Maulik D., Yarlagadda P., Youngblood J.P., Ciston P., (1990). The diagnostic efficacy of the umbilical arterial systolic/diastolic ratio as a screening tool: a perspective blinded study. Am. J. Obstet. & Gynecol., 162(6): 1518-1525.

Maulik D., Yarlagadda P., Downing G., (1990b). Doppler velocimetry in obstetrics. Am. Clin. Obstet. & Gynecol., 17(1): 163-186.

Maulik D., (1993). Hemodynamic interpretation of the arterial Doppler waveform. Ultrasound in Med. & Biol, 3(3): 219-227.

Mcneill G., Anderson D., (1992). Artificial neural network. A DACS State-Of-The-Art Repory (Data analysis center for software). Utica, New York, 2-70

Mine M., Nishio J., Nakai Y., Imanaka M., Ogita S., (2001). Effect of umbilical arterial resistance on its arterial flow velocity waveforms. Acta. Obstet. & Gynecol. Scand., 80 (4): 307-310.

Mires G., Dempster J., Patel N., Crawford J. (1987). The effect of foetal hear rate on umbilical artery flow velocity waveforms. Br. J. Gynecol. & obstet., 94(7): 665-669.

Mulders L.G., Muijsers G.J., Jongsma H.W. (1986). The umbilical artery blood flow velocity waveform in relation to foetal breathing movements, foetal heart rate and foetal behavioural states in normal pregnancy at 37 to 39 weeks. Early Hum. Dev., 14 (3-4): 283-293.

Myers LJ. Mathematical modeling of foetal arterial blood flow. PhD thesis. University of Cape Town. August 2001. This project was published in:
Myers L.J., Capper W.L., Cowper J.G., (2002). A transfer function-based mathematical model of the foetal-placental circulation. Ultrasound in Med. & Biol., 28(11/12): 1421-1431.

Nicolaides K.,Rizzo G.,Hecker K., Ximens R., (2002). Diploma in foetal medicine & ISUOG educational series: Doppler in Obstetric. The last accessed 2004/11/25.
http://www.centrus.com.br/DiplomaFMF/SeriesFMF/doppler/capitulos-html/chapter_03.htm

Pijneborg R., Bland J.M., Robertson W.B., Brosens I., (1983). Uteroplacental arterial changes related to interstitial trophoblast migration in early human pregnancy. Placenta, 4(4): 397-414.

Salafia C.M., (1997). Placental pathology of fetal growth restriction. Clin. Obstet. & Gynecol., 40 (4): 740-749.

Salafia CM., Pezzullo JC., Minior VK., Divon MY. (1997). Placental pathology of absent and reversed end-diastolic flow in growth restricted fetuses. Clin. Obstet. & Gynecol., 90 (5): 830-863.

Sameem A., Sapiyan B., Yong Z., Prasad U., Mohd I., Wahid A., (2002). Backpropagation neural network for medical prognosis: A comparison of different training algorithms. Last accessed 2004/06/10.
URL http://www.tech.plym.ac.uk/spmc/biomedical/biomedical_nnets.html

Ramsey E.M., Corner G.W., DonnerMW (1963). Serial and cineradioangiographic visualization of maternal circulation in the primate (hemochorial) placenta. Am. J. Obstet. & Gynecol.,86: 213–225.

Reed R.D.,Robert J., (1999). Neural Smithing: Supervised Learning in Feed forward Artificial Neural Networks. Cambridge, MA: MIT Press.

Robert A. Chipman, (1969). Theory and problem of transmission lines. Schaum's outline series, McGraw-Hill Book Company, USA.

Rosemary S., Thompson and Brain J, Trudinger (1989). Doppler waveform pulsatility index and resistance, pressure and flow in the umbilical placental circulation: an investigation using a mathematical model. Ultrasound in Med. & Biol, 16 (5): 449-458.

Rosenfeld C.R., (1992). Regulation of the placental circulation. In: Polin R.A., Fox W.W. (eds) Placenta. Saunders, Philadelphia USA, 56-61.

Ruissen C.J., Drongelen V., Hoogland H..J., Jager W., Hoeks A.P., (1990). Characteristics of the umbilical artery velocity waveform as a function of measurements site. Obstet. & Gynecol. Invest., 30 (4) : 212-216.

Rumelhart D.E., McClelland J.L., (1986). Parallel Distributed Processing: Explorations in the Microstructure of Cognition: Foundations.Vol. 1, MIT Press, Cambridge, MA, USA.

Sonesson S.E., Fouron J.C., Drblik S.P., Tawile C., Lessard M., Skoll A., Guertin M.C., Duchharme G.R., (1993). Reference values for Doppler velocitric indices from the foetal and placental ends of the umbilical artery during normal pregnancy. J. Clin. Ultrasound, 21(5): 317-324.

Stergiou C., Siganos D., (1996). Neural networks online. Last accessed 2004/11/25 URL http://www.doc.ic.ac.uk/~nd/surprise_96/journal/vol4/cs11/report.html

Stuart P. (1992). An assessment of the role of Doppler ultrasound velocity waveform analysis of the umbilical artery in the diagnostic of foetal distress in labour. MSC thesis, University of Cape Town, 30:50

Surat R., Admson S.(1996). Downstream determinants of pulsatility of the mean velocity waveform in the umbilical artery as predicted by a computer model. Ultrasound in Med. & Biol, 22(6) : 707-717.

The MathWorks, Inc. (2004). Neural network toolbox. Last accessed 2004/11/25 URL http://www.mathworks.com/access/helpdesk/help/toolbox/nnet/nnet.html

Thompson R.S., Stevens R.J. (1989). Mathematical model for interpretation of Doppler velocity waveform indices. Med. Biol. Eng. Comput., 27(3): 269-276.

Thompson R.S., Trudinger B.J., Cock C.M., (1986). A comparison of Doppler ultrasound waveform indices in the umbilical artery –I. Indices derived from the maximum velocity waveform. Ultrasound in Med. & Biol, 12(11): 835-844.

Trudinger B.J., Giles W.B., Cook C.M., (1985a). Uteroplacental blood flow velocity-time waveforms in normal and complicated pregnancy. Br. J. Obstet. & Gynaecol., 92(1): 39–45.

Trudinger B.J., Giles W.B., Cook C.M., Bombardieri J., Collins L., (1985b). Fetal umbilical artery flow velocity waveforms and placental resistance: clinical significant. Br. J. Obstet. & Gynecol, 92 (1): 23-30.

Trudinger B.J., (1987). The umbilical circulation. Semin Perinatol, 11(4): 311-321.

Trudinger BJ., Giles WB. (1996). Elaboration of stem villous vessels in growth restricted pregnancies with abnormal umbilical artery Doppler waveforms. Br. J. Obstet. & Gynaecil., 103 (5) : 487-496.

Yarlagadda P., Willoughby L., Maulik D., (1989). Effect of foetal heart rate on umbilical arterial indices. Am. J. Ultrasound in Med. & Biol, 8(4): 215-218.